NATIONAL ADVISORY COMMITTEE FOR AERONAUTICS

TECHNICAL MEMORANDUM 1254

SYSTEMATIC MODEL RESEARCHES ON THE STABILITY LIMITS OF THE DVL SERIES OF FLOAT DESIGNS

By W. Sottorf

Translation of "Systematische Modelluntersuchungen über den tauchstampffreien Stabilitätsbereich des DVL-Einheitsschwimmers." Jahrbuch 1942 der Deutschen Luftfahrtforschung.

Washington
December 1949

NATIONAL ADVISORY COMMITTEE FOR AERONAUTICS

TECHNICAL MEMORANDUM 1254

SYSTEMATIC MODEL RESEARCHES ON THE STABILITY LIMITS OF THE DVL SERIES OF FLOAT DESIGNS*

By W. Sottorf

SUMMARY

To determine the trim range in which a seaplane can take off without porpoising, stability tests were made of a plexiglas model, composed of float, wing, and tailplane, which corresponded to a full-size research airplane. The model and full-size stability limits are in good agreement. After all structural parts pertaining to the air frame were removed gradually, the aerodynamic forces replaced by weight forces, and the moment of inertia and position of the center of gravity changed, no marked change of limits of the stable zone was noticeable. The latter, therefore, is for practical purposes affected only by hydrodynamic phenomena. The stability limits of the DVL family of floats were determined by a systematic investigation independent of any particular seaplane design, thus a seaplane may be designed to give a run free from porpoising.

SYMBOLS

A	aerodynamic lift, kilograms
A^*	hydrodynamic lift, kilograms
G	flying weight, kilograms
F	wing area, meters^2
J_y	pitching moment of inertia, meter kilograms second^2
f_y	radius of gyration, meters
b_{St}	beam at step, meters
b_{nat}	breadth of pressure surface, meters
b	wing span, meters
l	length of hull, meters
t	rise of center of gravity, meters

*"Systematische Modelluntersuchungen über den tauchstampffreien Stabilitätsbereich des DVL-Einheitsschwimmers." Jahrbuch 1942 der Deutschen Luftfahrtforschung, pp. I 451 - I 465.

v	speed, meters per second
F	Froude number
f	frequency, 1/S
q	dynamic pressure (air or water), kilograms per meter^2
c_a	aerodynamic lift coefficient $\left(\frac{A}{Fq_l}\right)$
$c_a{}^*$	beam loading $\left(\frac{A^*}{\gamma b_{St}{}^3}\right)$
c_B	hydrodynamic lift coefficient $\left(\frac{A^*}{qb_{St}{}^2}\right)$
α^*	trim or attitude of keel tangent at step to horizontal, degrees
α	wing angle of attack, degrees
ζ	keel angle, degrees
λ	scale
η, η_k	elevator or flap deflection
ρ	density, kilograms seconds^2 per meter^4
γ	specific weight, kilograms per meter^3

I. INTRODUCTION AND RANGE OF INVESTIGATION

By porpoising is understood an oscillation occurring, even in calm water, during the landing and take-off of seaplanes, which combines an angular oscillation in pitch with a vertical movement of the center of gravity. The disturbance is sometimes so great that the only possible preventative - damping control from the elevator - is of no use. German seaplanes have suffered little from this phenomenon - much less so than prewar English aircraft. In England clarification of the nature of, and cure for, porpoising has been attacked by using dynamically similar models. (See references 1 and 2.)

Our researches confirm those made in England which show that all seaplanes have a definite zone of stable attitudes similar to that shown in figure 1. The position of the upper and lower limits of this stability region varies from aircraft to aircraft, but there are several features common to all aircraft. The limits diverge with increasing speed. The lower limit is highest near the hump - where the stable zone is narrowest - and a seaplane having too high or too low an attitude there will be almost certain to porpoise. Just before take-off, crossing the upper limit may lead to severe porpoising causing the seaplane to bounce clear of the water. On the other hand, the amplitude of porpoising may be limited by the influence of the afterbody. The real danger point occurs at high speed in the lower limit, where a porpoise, building up rapidly, may cause the bow to dig in. This usually leads to total loss of the aircraft. Such a case has been encountered on the latest English flying boat - Short "Empire."

As stated above, German seaplanes in general are in no danger from porpoising provided they do not encounter a large disturbance. This stability is dependent on

(a) The position of the stability limits

(b) Any factors which may affect the attitude

Of particular significance is the determination of stability limits for the DVL family of floats giving the most suitable dimensions for any hull, that is, length, deadrise, and beam loading (reference 3). The primary purpose of this investigation, however, is, by systematic stability tests, to enable the stability of any run to be forecast with accuracy.

In addition it is necessary to find if the influence on stability of the aerodynamic components of a seaplane combined with center-of-gravity shift and change of moment of inertia is sufficiently small to be neglected.

The groundwork for the foregoing tests was established by a series of tests on a model consisting of float plus wing and tail surfaces. This model was similar to a Vought V85 fitted with a DVL-family float (reference 4). By altering the moment of inertia, replacing the aerodynamic forces by weights, and by moving the center of gravity the influence of these factors on stability was investigated in the tank.

In a further research the influence of deadrise angle was determined by testing a series of unwarped planing surfaces having different deadrise angles. In addition, tests were made on six models

of two float families with keel angles of 130° and 140° to determine the stability limits over the attainable attitude range. Finally an examination was made of the effect of the afterbody by tests on a series of forebodies alone.

II. RESEARCH PROCEDURE

The apparatus used in the tests is illustrated in figure 2. The model is carried forward and under the carriage in order to eliminate as far as possible the effects of air-flow interference from the carriage (reference 5).

The model is constructed of plexiglas throughout. Wing and tail surfaces for the float under test are attached to a framework on the float. Movable weights are used to change the total weight and moment of inertia. The float is divisible into two parts at the step, thus allowing variation of the forebody-afterbody combination and step height. Plexiglass construction offers the following advantages:

(a) Being transparent it allows observation of the flow over the bottom.

(b) It compares favorably with balsa construction for weight and strength.

(c) It is not subject to distortion and is water resisting.

This last quality in particular has facilitated lengthy tank researches. The model (fig. 2) is towed at the center of gravity s by way of a rod f_1 which is free to move in a vertical direction. In addition the model is free to pitch. A second guide f_2 limits directional rotation to $\pm 1°$ and provides a stop for excessive pitch oscillation which otherwise might damage the model. The rise t and the attitude α^* of the float can be read during a test from scales mounted above the model. For greater accuracy the results are also recorded on the carriage by way of two wires in tension z_1 and z_2. A third wire z_3 transmits the relieving load when this is used in place of aerodynamic lift.

III. PRELIMINARY RESEARCH

The preliminary tests were made under similar conditions to those described in reference 4 with the single-float Vought V85 aircraft

which is used as a test bed for the DVL float family. The beam of the models is $b_{St} = 0.2$ meters and the model scale $\lambda = 5.5$.

Figure 3 shows the results from these preliminary tests. The models were tested at four different speeds, the lowest speed being slightly above hump speed and the highest near take-off speed.

Three symbols are used:

+ stable, no tendency to oscillate, positive damping

o borderline, slight oscillation, no damping

● unstable, undamped oscillation

To prevent the model propoising by entering the unstable region before it reaches the test speed, it is held in the carriage during the run up and then released with elevators set to give the attitude required. By this means the model in falling onto the water is given a disturbance of 2° or 3° within the stable region and this, combined with the slight residual wave motion in the tank, is considered to give sufficient disturbance.

Figure 4 gives a number of individual records and photographs from these tests. The angle given α^* is the angle at which the oscillation is initiated. This does not, in general, agree with the mean attitude of porpoising α^*_{mean}. It has been shown that α^*_{mean} within the stable region is smaller in the upper stability region and larger in the lower stability region than α^*. It can be seen that attitude and rise oscillations are in phase (and of similar frequency) and that the maximum rise coincides with the maximum attitude. This corresponds to the equilibrium position on the water provided that the inertia forces are small. The introduction of a positive increase in attitude increases the hydrodynamic impulse; the equilibrium of forces is maintained by a vertical center-of-gravity rise resulting in a reduction of the effective pressure area. A periodic repetition of this process leads to porpoising.

The boundary zone between stable and unstable regions proved to be very small indeed and the accuracy of the limits given is reckoned to be $\pm\frac{1}{4}^\circ$.

IV. EFFECT OF ALTERATIONS TO THE MODEL

(a) Alteration of Moment of Inertia

By displacing the trim weights on the model balance arm, the moment of inertia J_y was increased in two steps by 42 percent and 97 percent to find the influence of an excessive moment of inertia on stability.

In figure 5 the nondimensional coefficient

$$C_{iy} = \frac{i_y}{\sqrt[3]{\frac{G}{\gamma}}}$$

has been plotted as a function of weight G for a number of aircraft, and it can be seen that the moment of inertia of the full-scale V85 is representative of modern practice and that an increase of 97 percent brings the moment of inertia well above normal.

Comparison with the preliminary tests shows that the stable conditions are unaffected by these changes in moment of inertia. In the unstable region the amplitude of oscillation increases with increase in moment of inertia, and points which are on the borderline (zero damping) at low and intermediate moments of inertia become unstable at high moments of inertia. For this reason, the limits were plotted so that the border points (o) fell within the unstable region. Extrapolating the frequency for a model moment of inertia corresponding to complete dynamical similarity by using the formula obtained for the physical pendulum,

$$f^2 = \frac{c}{J} \quad (c = 0.638 \text{ average})$$

in conjunction with the three measured frequencies gives a model scale frequency f_M of 2.05. Lechner estimated that under similar conditions $f_{\text{full scale}} = 0.85 = f_H$

Then scaling down dynamically

$$f_M = f_H \sqrt{\lambda}$$

$$= 2.35\ f_H = 2.00$$

which agrees with the measured value.

(b) Change of Mass and Damping

Replacement of wing lift by weights.- The lifting surface was removed and the original weight and moment of inertia restored. In conjunction with the elevator positions obtained from the basic research, the float positions corresponding to various wing lifts were obtained by suitable adjustment of relieving weights (through the wire z_3 shown in figure 2). This replacement of wing lift by weight did not influence the stability limits. In the unstable region the porpoising amplitude was increased as a result of the absence of wing aerodynamic damping.

Doubling the tail-surface area.- At low water speed the elevator has insufficient power to trim the aircraft such that the unstable points can be determined, and weights are used instead. With twice the tail area these points can be reached without resort to weight movement. The stability limits are not affected, but there is a proportionately small decrease in the porpoising amplitude owing to the greater damping effect.

Replacement of the elevator moments by weights.- The tail was also removed and replaced by weights; no effect on the limits was noted apart from a slightly increased amplitude of oscillation because of the decrease in aerodynamic damping (fig. 6).

(c) Center-of-Gravity Movement

A center-of-gravity range from $\frac{1}{4}b_{St}$ behind the step to $\frac{1}{2}b_{St}$ in front of the step was tested over the whole speed range. This center-of-gravity movement covers the center-of-gravity limits of most existing seaplanes.

The curves of figure 7 show that the center-of-gravity movement also has no effect on the stability limits.

An effect of vertical movement of the center of gravity is hardly to be expected from these results, and was therefore not investigated.

(d) Effect of Loading

The foregoing alterations to the model indicate that the stability limits are independent of any changes in the superstructure and are only influenced by hydrodynamic effects on the float. Hence the effect of loading can be investigated on the model without lifting surface and at a constant load. The loading can then be varied to cover the whole weight range required.

In figure 8 the stability limits for loadings $c_a^* = 0.37$ to 1.85 are given. The tailplane was retained and the attitude varied by altering the

elevator deflection. The above loads are influenced by the tailplane lift; a correction has been made for this and the limits reduced to constant c_a*.

Figure 8 shows that with increasing load both upper and lower limits move towards higher attitudes by approximately equal amounts.

If, as in figure 9, α* is plotted against the hydrodynamic lift coefficient $c_B = \frac{A^*}{qb_{St}^2}$, determined in reference 6, it is apparent that the highspeed lower-stability curves, where the stern is not wetted and at which the influence of Froude number is negligible, coincide. The spreading of the stable zone below the hump appears in figure 9 as a branch curve deviating from the direction of the mean line.

The limits for the preliminary research have been interpolated from figure 8 and they agree with the limits obtained by direct measurement, figure 10.

V. COMPARISON BETWEEN MODEL AND FULL SCALE

Comparison between model and full scale is given in figure 11. Since, as has been shown already, the limits are sensitive to load on the water, the model scale results were corrected for increase in lift due to propeller thrust component and slipstream.

The agreement between the two is good. On the lower limit, the difference is nowhere greater than $\frac{1}{2}^\circ$. On the upper limit the corresponding curves diverge at low speed. It may be that at this point premature porpoising has occurred as a result of wing stall on the full-scale aircraft since $c_{a_{max}}$ occurs at $\alpha^* = 10^\circ$ full scale and not until $\alpha^* = 15^\circ$ on the model. The agreement between frequencies has been noted in section IV(a).

VI. SYSTEMATIC INVESTIGATIONS WITH PLANING SURFACES, FOREBODIES, AND SIX DVL FLOATS

(a) Planing Surfaces

To investigate the effect of deadrise alone, four longitudinally unwarped planing surfaces with keel angles of 130°, 140°, 160°, and 180° and 0° (fig. 12) were tested - the first two correspond to the angles of deadrise on the DVL float family. The results from these planing surfaces are

plotted in figure 15. The constant loadings chosen - uncorrected for tail lift - correspond to those given in figure 22 for the floats; the speed range covered was also similar.

At first glance it is obvious that the character of the lower limits and their sensitivity to load confirm the results already obtained. At low speed there exists - depending on the length of the surface and provided a sufficiently great nose-down moment can be achieved - a second limit below the primary one. The two limits meet at a speed slightly below the hump speed. But, since at this speed the limits are greatly dependent on the effect of the afterbody, this secondary limit is of no practical significance.

There is no upper limit. The attitude of the planing surface at various loads and speeds was increased to 20° - in which case the wetted length was 20 to 30 mm - without encountering porpoising. However, the flat surface was very sensitive to a disturbed water surface and a pure vertical oscillation occurred at attitudes from 3° to 9° - depending on the loading - above the stable attitude. The amplitude of this oscillation increased with increase in attitude (fig. 17); at low weight and high speed the trailing edge is thrown off the water. With perfectly undisturbed water the oscillation does not appear. The surfaces with deadrise showed no tendency to oscillate under similar conditions.

Figure 16 gives the limits interpolated for dimensionless speed and load coefficients (corrected for tail lift).

The surfaces with deadrise gave similar results to the flat surface. Figure 18 gives curves showing the variation of stability limits with load for three Froude numbers with deadrise as a parameter. There is little difference between the limits for the surfaces with deadrise but, considering the accuracy with which the whole series of tests has been performed, there is a tendency, somewhat ill defined it is true, towards raising of the upper limit with increase in deadrise. Following this trend, the limit for the flat surface is the lowest of the set. The distinction here is, however, much greater and varies between 0.5° and 2.0°, possibly a result of the sensitivity to water conditions noted previously.

(b) Forebodies

The forebodies of the DVL float family B which have a keel angle of 130° (fig. 13) were subjected to the same program of tests as the planing surfaces and complete floats (fig. 22). The results are given in figures 19 and 20.

These forebodies differ from the planing surfaces in having (1) increased deadrise towards the bow by reason of the warp on the

hull and (2) flare at the chine. The influence of these factors on stability is clearly shown in the comparison between planing surfaces and forebodies.

As with the planing surfaces, there is no upper limit (attitude range covered = 20°) (fig. 21). With the shortest forebody - DVL 17, figure 19 - the lower limits are from 0.5° to 2° higher over the whole speed range; the smaller the attitude the longer is the wetted surface and more of the strongly warped bow is subject to pressure. At low loads and high water speed, the difference is accentuated. The warping has obviously the greatest influence since the change in deadrise has already been shown to be of comparative unimportance and the chine flare reducing as it does the pressure area is an ameliorating factor.

The forebody of intermediate length - DVL 18 - which was tested only over a limited speed range at high load shows that for $c_a^* = 1.25$ and $F = 4$ the limits are coincident and that at higher load the forebody is somewhat better than the corresponding planing surface. This tendency was also apparent in the tests on DVL 17 where the difference between forebody and planing surface limits is decreased as the load increases.

As would be expected, the long forebody - DVL 19 - shows an even greater improvement at high load. At low load and high speed the planing surface is still the more stable but the difference between the two is much less than with the shortest forebody.

This variation with high and low load and with long and short forebodies caused by bow warp should be corroborated by further research.

(c) DVL Float Family

Family B, DVL 17, 18, and 19. $\zeta = 130°$
Family A, DVL 1a, 8, and 7. $\zeta = 140°$

The range of weights and speeds covered is given in figure 22.

In figures 23 to 25 the results of the measurements on Family B (fig. 14) are plotted in the form of curves of α^* as $f(v)$ with load G as a parameter. There is now an upper limit as a result of stern wetting, which is initiated somewhat below the upper limit.

For the short and long hulls the frequency of the porpoising oscillation at each experimental point has been plotted in addition to the stability limits (figs. 23 and 25). It can be seen that on the lower limit the frequency at high speed is almost double that at the hump. On the upper limit the difference is not so great. The frequency also increases with increase in weight and length, and is greater at the upper limit than at the lower. These results confirm the contention made earlier that the frequency of porpoising once it has started is greatly dependent on the moment of inertia. For ease of interpolation the limits have been plotted nondimensionally using α^* as a function of c_a^* with F as parameter and α^* as function of F with c_a^* as parameter (figs. 26 - 28).

In figures 29 to 31 is given the relationship between the limits and c_B^*. At high speed the curves of lower limit can be collapsed with a scatter of less than 0.5°. For the upper limits the scatter is less than 1°. This result indicates that at high Froude number when the planing condition has been reached the transition from the stable to the unstable state occurs at a given value of $\frac{A^*}{qb_{St}^2}$ and wetted length and is independent of Froude number.

Although, as is already established, the afterbody initiates the upper limit, it has a stabilizing effect, on the lower limit. In figures 23 to 25 the limits for the forebodies can be compared with the limits for the complete hulls. The afterbody lowers the limits in the region of the first hump so long as it is wetted. After the afterbody is clear, the limits coincide.

Float family A gave similar results to family B.

A comparative plot of the mean limits for these two families (fig. 32) shows that for the lower limits at high speed - low c_B - the DVL 1a with less deadrise is better than DVL 17. At lower speeds and high loads the DVL 17 shows up to best advantage. The differences between DVL 8 and 18 and DVL 7 and 19 are very slight, with the sharper keels somewhat better. On the upper limits the floats with the greater deadrise have the higher limits. The effect of $\frac{l}{b_{St}}$ ratio is not very obvious in this plot except in the hump region where the shortest hulls have a slightly higher, and lower limit. The ameliorating effect of increasing the $\frac{l}{b_{St}}$ ratio is more clearly defined in figure 33, which shows the maximal attitudes of the lower limits for several loads plotted against $\frac{l}{b_{St}}$.

VII. METHODS FOR WIDENING THE STABILITY REGION

The foregoing stability diagrams will give information for any projects based on the DVL float family. Even for designs somewhat different from this series the results will give sufficiently accurate information; for example, the deadrise has little effect, and the strength of the afterbody affects only the upper limit.

Widening the stability limits in cases where the attitude approaches the limits and for various reasons cannot be altered may be accomplished by the following means:

(a) Upper Limit

To make a short take-off the seaplane may be pulled off sharply thereby running into the upper limit. By using afterbody auxiliary steps from 0.01 to $0.02b_{St}$ deep (fig. 34), this limit can be raised as much as 3°. The optimum condition is reached when the tangential flow from the forebody is deflected by the auxiliary steps producing a stabilizing force (fig. 35). In addition there is a considerable reduction in resistance confirmed by full-scale tests.

(b) Lower Limit

By lowering the afterbody at the rear step or by utilizing a hook, the effect of the afterbody at the hump can be increased and the limit thereby lowered. This measure will, of course, result in a simultaneous lowering of the upper limit near take-off.

The whole lower limit can be lowered without affecting the upper limit by a slight concave keel camber immediately forward of the main step. Earlier experiments (reference 7) have shown that with a concave keel the center of pressure is moved nearer to the rear of the pressure area; hence the wetted area for a given weight is reduced and the resistance and spray characteristics improved.[1] Since the resultant

---

[1]This method was not pursued any further at the time because of the instability that was found. The results of that investigation do not, however, contradict the results obtained here as it was only concerned with flat surfaces. Without deadrise such a planing surface (see section VI(a)) particularly with longitudinal curvature, is very sensitive to water surface conditions - the surface with deadrise is not.

hydrodynamic lift is moved nearer the step, the running attitude is reduced. Hence, by a supplementary investigation a suitable combination of camber, step position, and center-of-gravity position must be found. In figure 36 the stability limits from three cambered hulls (as shown) are compared with the corresponding results for an uncambered hull (keel angle 130°, c_a* = 1.5 and 2). It can be seen that limits are moved in proportion to the angle at the step (5° 44' and 2° 52' investigated) while the radius and length of the hook (R = 10, 20 and $40b_{St}$ and l = 1 and $2b_{St}$) affect the limits only insofar as they change the angle at the step. As the load is reduced or the dynamic pressure increased, the change in attitude approaches the value of the step angle. Further research is required on this subject to determine a suitable camber.

VIII. CONCLUSIONS

Porpoising is an oscillation which occurs during the landing and take-off of a seaplane and which may lead to total loss of the aircraft.

An initial investigation was made with a plexiglas model, comprised of a float, wing, and tail, which was dynamically similar to the Vought V85 fitted with a DVL-family float. The model and full-scale give similar results for the stable regions. The limits of this region diverge with increasing speed.

The following alterations were found to have no noticeable effect on the position of the limits: alteration of moment of inertia, center-of-gravity position, replacement of the aerodynamic lift from the wing and tail surfaces by weights. These alterations have some effect on the behavior within the unstable regions.

Load on the water has, however, a considerable influence on the position of the limits. Both limits are moved to higher attitudes with increase in load. The limits determined for a series of weights can be used to interpolate the limits corresponding to any given wing lift.

There followed an investigation into the effect of deadrise angle with unwarped planing surfaces. Comparison with tests made on a series of forebodies of varying $\frac{l}{b_{St}}$ ratio shows the effect of warp, and further comparison with tests on two families of complete hulls gives the afterbody effect.

A seaplane with forebody alone has no upper-limit instability up to the maximum practicable attitude. If a flying boat shows instability at the upper limit, this can be cured by altering the afterbody only - increasing the afterbody keel angle. For the lower limit the afterbody is stabilizing near the hump, that is, so long as it is wetted, and as a result the lower limit, which rises sharply with decrease in speed till it reaches the hump, falls away again.

When no other means are available the limits can be widened if necessary by

(a) The addition of small auxiliary steps on the afterbody which will raise the upper limit

(b) Lowering the afterbody or hooking the rear step which will lower the lower limit at the hump

(c) Making a slight concavity in the keel immediately forward of the step thereby lowering the complete lower limit

This last alteration affects the running attitude so that a suitable compromise must be made between step position, center-of-gravity position, and degree of concavity.

With the working diagrams of the DVL float families presented herein at hand the designer can now design a seaplane with a take-off or landing run free from porpoising.

Translated by
J. A. Hamilton
Marine Aircraft Experimental Establishment, Felixstowe.

REFERENCES

1. Perring, W. G. A., and Hutchinson, J. L.: Full Scale and Model Porpoising Tests of the Singapore IIC. R & M No. 1712, British A.R.C., 1936.

2. Coombes, L. P., Perring, W. G. A., and Johnston, L.: The Use of Dynamically Similar Models for Determining the Porpoising Characteristics of Seaplanes. R & M No. 1718, British A.R.C., 1936.

3. Sottorf: Gestaltung von Schwimmwerken. Jahrbuch 1937 der Deutschen Luftfahrtforschung, p. I 309. (Available as NACA TM 860.)

4. Lechner: Untersuchungen über die dynamische Stabilität von Seeflugzeugen auf dem Wasser. Flugbaumeisterarbeit.

5. Sottorf: Start und Landung im Modellversuch. Jahrbuch 1938 der Deutschen Luftfahrtforschung, Ergänzungsband p. 396. (Available as British R.T.P. Translation No. 966.)

6. Sottorf: Analyse experimenteller Untersuchungen über den Gleitvorgang an der Wasseroberfläche. Jahrbuch 1937 der Deutschen Luftfahrtforschung, Erganzungsband p. I 320. (Available as NACA TM 1061.)

7. Sottorf: Versuche mit Gleitflächen, III. Teil. Werft, Reederei, Hafen (1933), Nr. 4/5. (Available as NACA TM 739.)

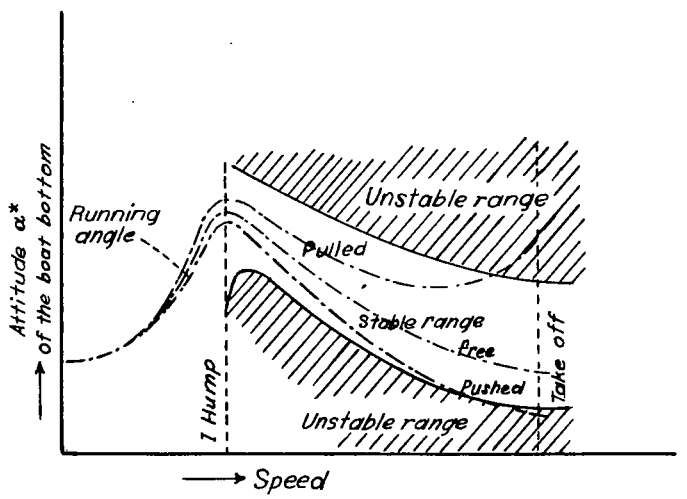

Figure 1.- Schematic representation of the position of the range free from porpoising.

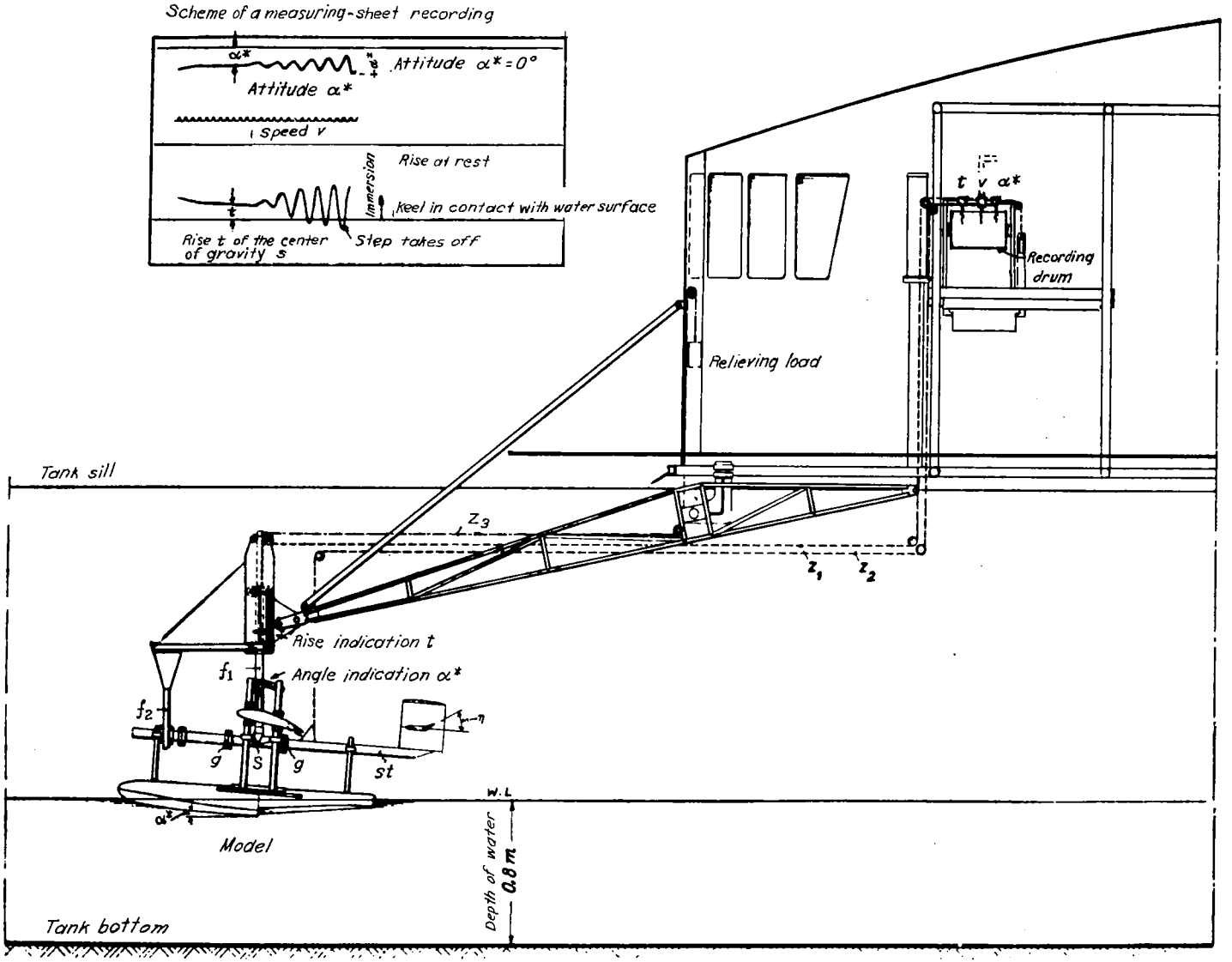

Figure 2.- Measuring apparatus for porpoising tests.

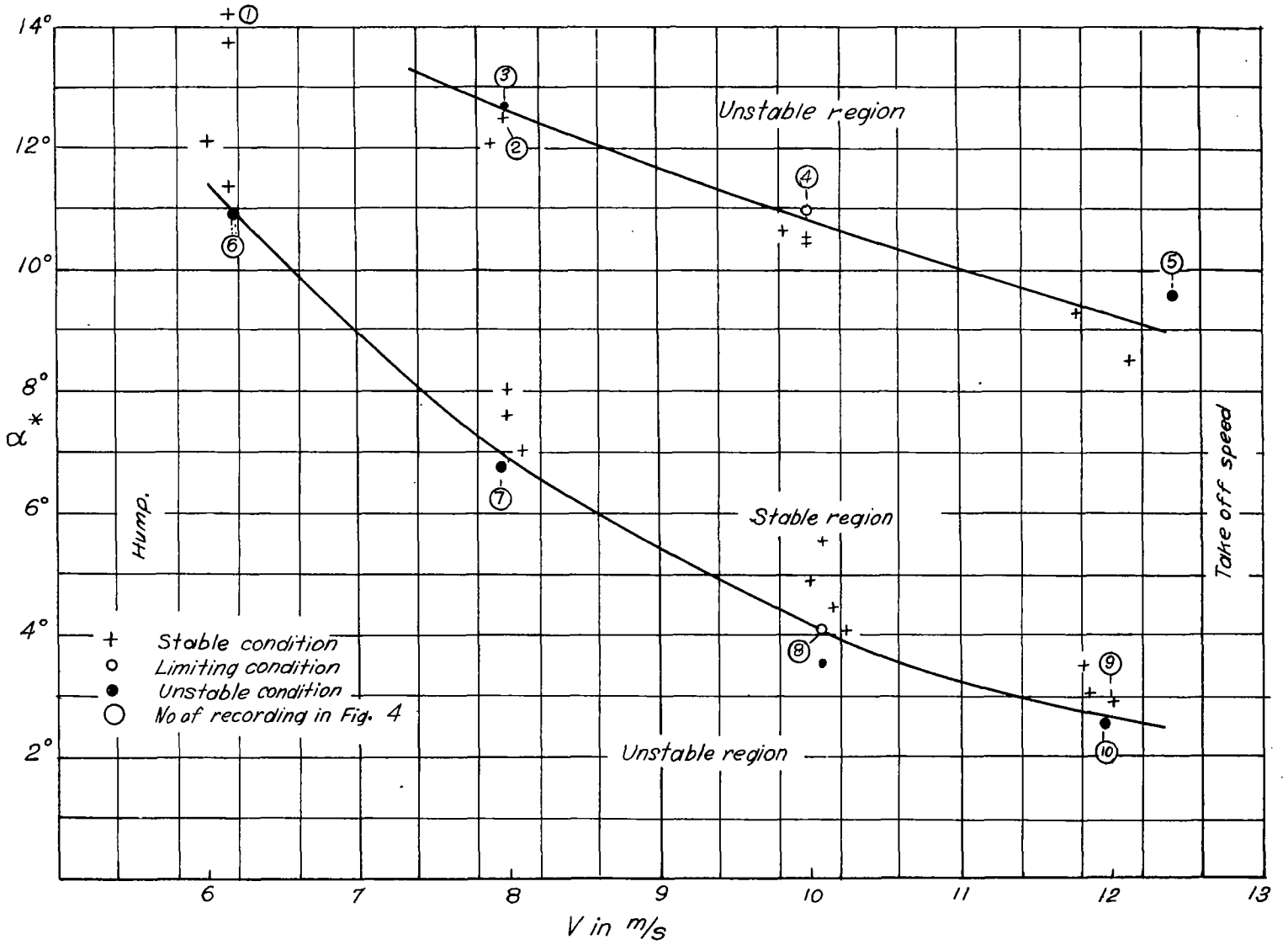

Figure 3.- Basic test. Float design DVL 18 with wing and tail plane.

(The numbers in the circles referring to parts of figure 4 were incorrect in the original version of this paper and have been corrected by the NACA reviewer.)

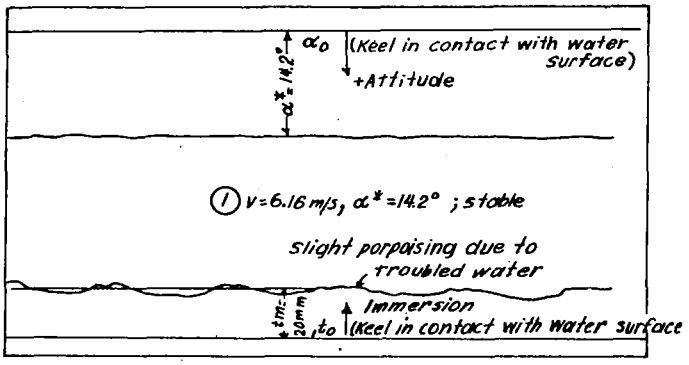

(a) 6m/s: Photograph figure 4(a) shows a stable run for $\alpha^* = 14.2^0$. A larger part of the afterbody still participates in the lift. The corresponding recording is No. 1 from figure 4. The mostly irregular surface waves remaining in the tank after several test runs in spite of wave damping the height of which has been registered with ±2 mm at rest cause a corresponding porpoising. The attitude is not influenced thereby. The upper unstable range is not included at this speed.

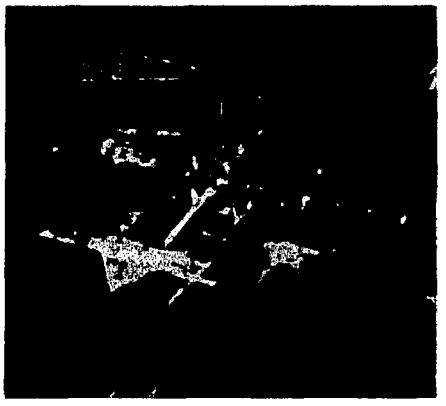

Figure 4(a)

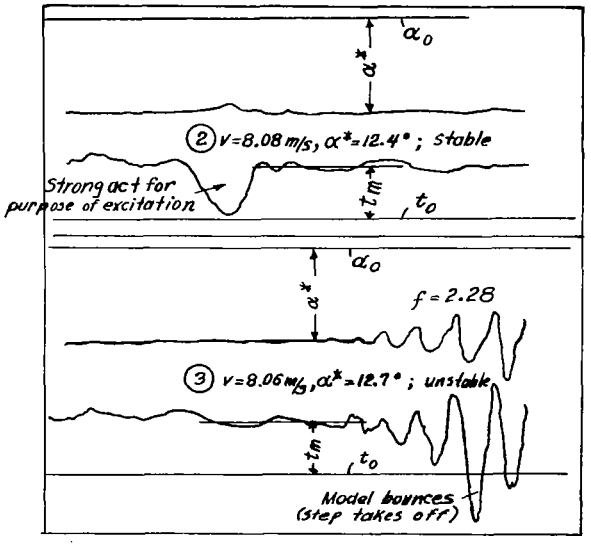

(b) 8m/s: Photograph figure 4(b) shows a stable run for $\alpha^* = 12.4^0$. The afterbody is still supporting. Recording No. 2 shows the strong damping at touch of the model. Recording No. 3 shows the oscillation occurring if the attitude is increased by only 0.3^0. The porpoising amplitude has, after only 4 oscillations, increased so much that the step takes off from the water. The afterbody remains in contact with the water; thus a rotation about an instantaneous point of rotation shifted far to the rear takes place.

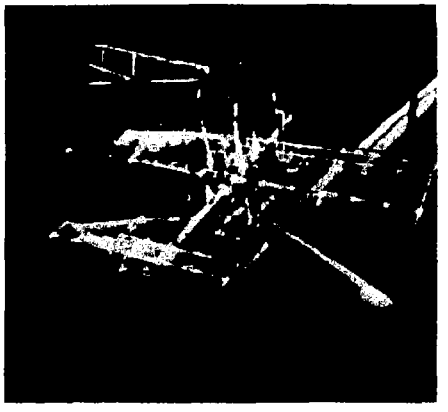

Figure 4(b)

Figure 4.- Recordings of rise t and attitude α^* for preliminary test.

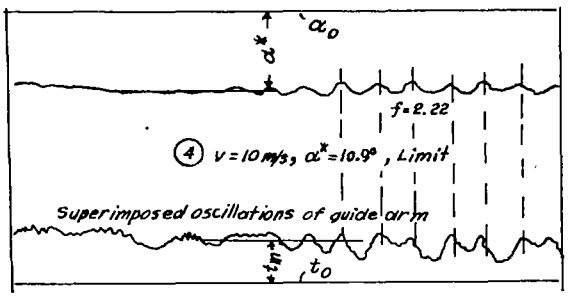

(c) 10m/s: Photograph figure 4(c) shows a stable run for $\alpha^* = 10.4^\circ$. The step is no longer loaded to its full width $(b_{nat} < b_{st})$, the afterbody is therefore under spray effect. The recording No. 4, $\alpha^* = 10.9^\circ$, is an example for a limiting condition. The amplitudes of porpoising and pitching oscillation remain constant. The frequencies of both oscillations are the same for all tests; largest attitude and highest position of the center of gravity always coincide.

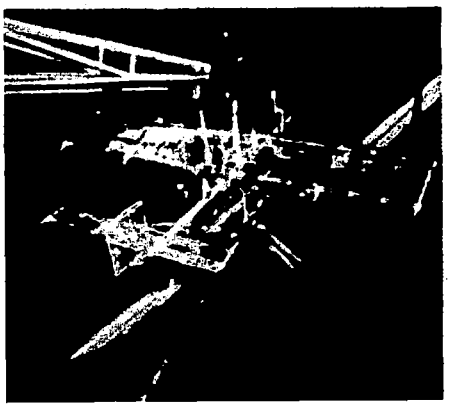

Figure 4(c)

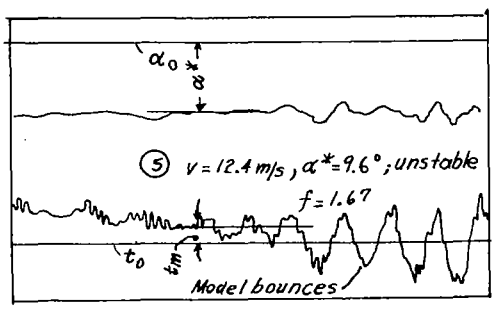

(d) 12m/s: Photograph figure 4(d) shows a stable run before taking off for $\alpha^* = 8.7^\circ$. Afterbody under strong splash effect. The recording No. 5 shows an unstable condition in which the model bounces heavily. Due to the limiting afterbody the amplitude of the pitching oscillation remains comparatively small with $\sim 3^\circ$.

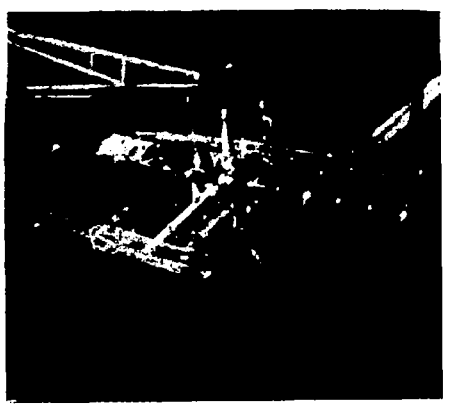

Figure 4(d)

Figure 4.- Continued.

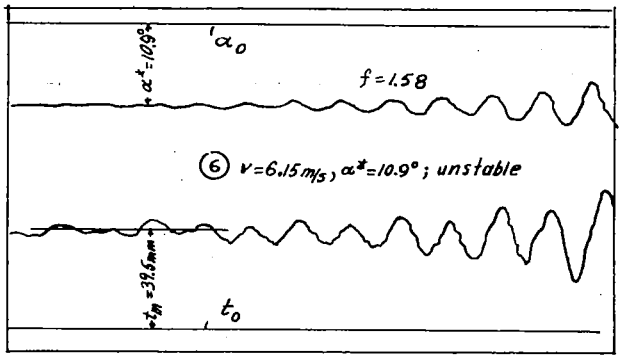

(e) 6m/s: Recording No. 6 shows an unstable condition in the range of the hump for $\alpha^* = 10.9^\circ$; the afterbody is still loaded. Since the unstable range here extends to high attitude, an airplane which overcomes the hump with a comparatively low attitude may in this range be excited porpoising which is damped only when the airplane, under further increasing speed, enters the stable range.

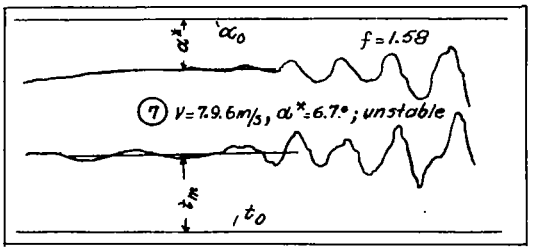

(f) 8m/s: Recording No. 7 shows an unstable condition for $\alpha^* = 6.7^\circ$, gliding condition proper. The afterbody limits the attitude for maximum porpoising.

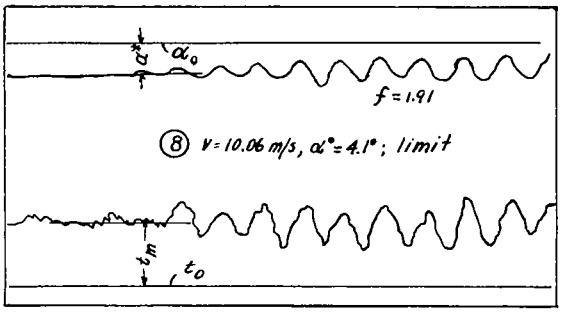

(g) 10m/s: Recording No. 8 shows once more a limiting condition; the model is in gliding condition proper; the afterbody is in contact with the water during the oscillation.

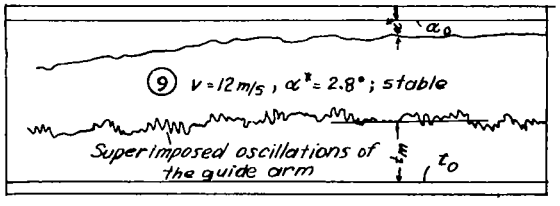

(h) 12m/s: Recording No. 9 shows a stable run for $\alpha^* = 2.8^\circ$. Recording No. 10 shows the most critical porpoising case which is registered if the attitude is reduced by only 0.3°. Already after 5 oscillations the model bounces, with the amplitude of the pitching oscillation increasing very greatly as well. Negative attitudes of the floats are attained and the bow digs in. In contrast, the mean attitude increases considerably and covers the entire stable range without occurrence of damping.

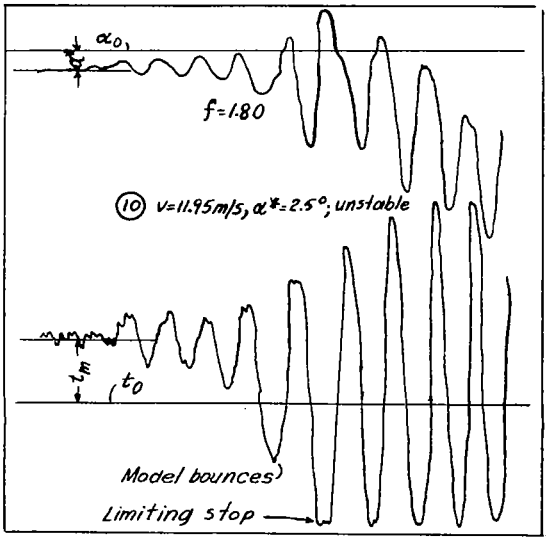

Figure 4.- Concluded.

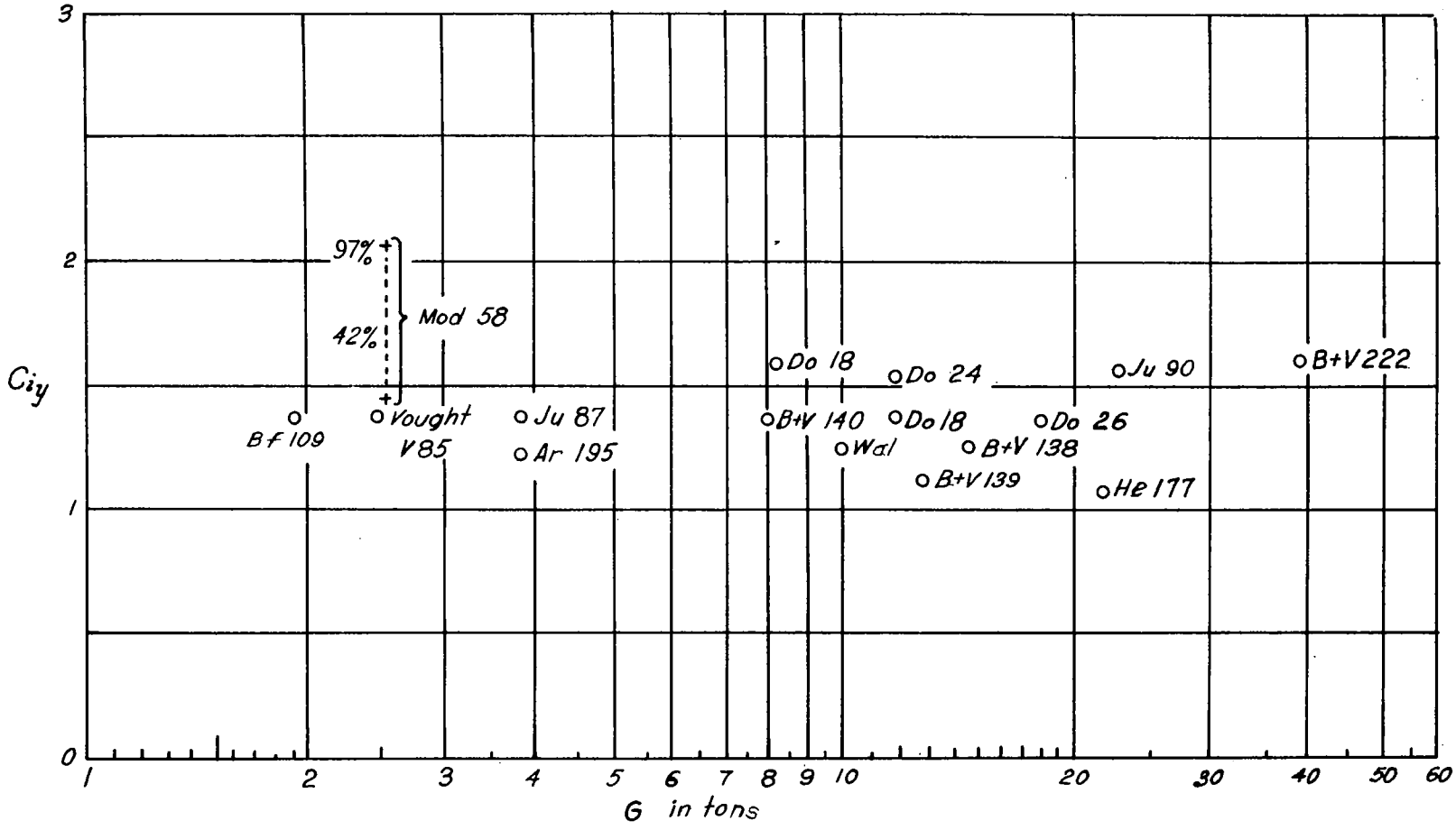

Figure 5.- Coefficient of the moment of inertia as a function of the flying weight.

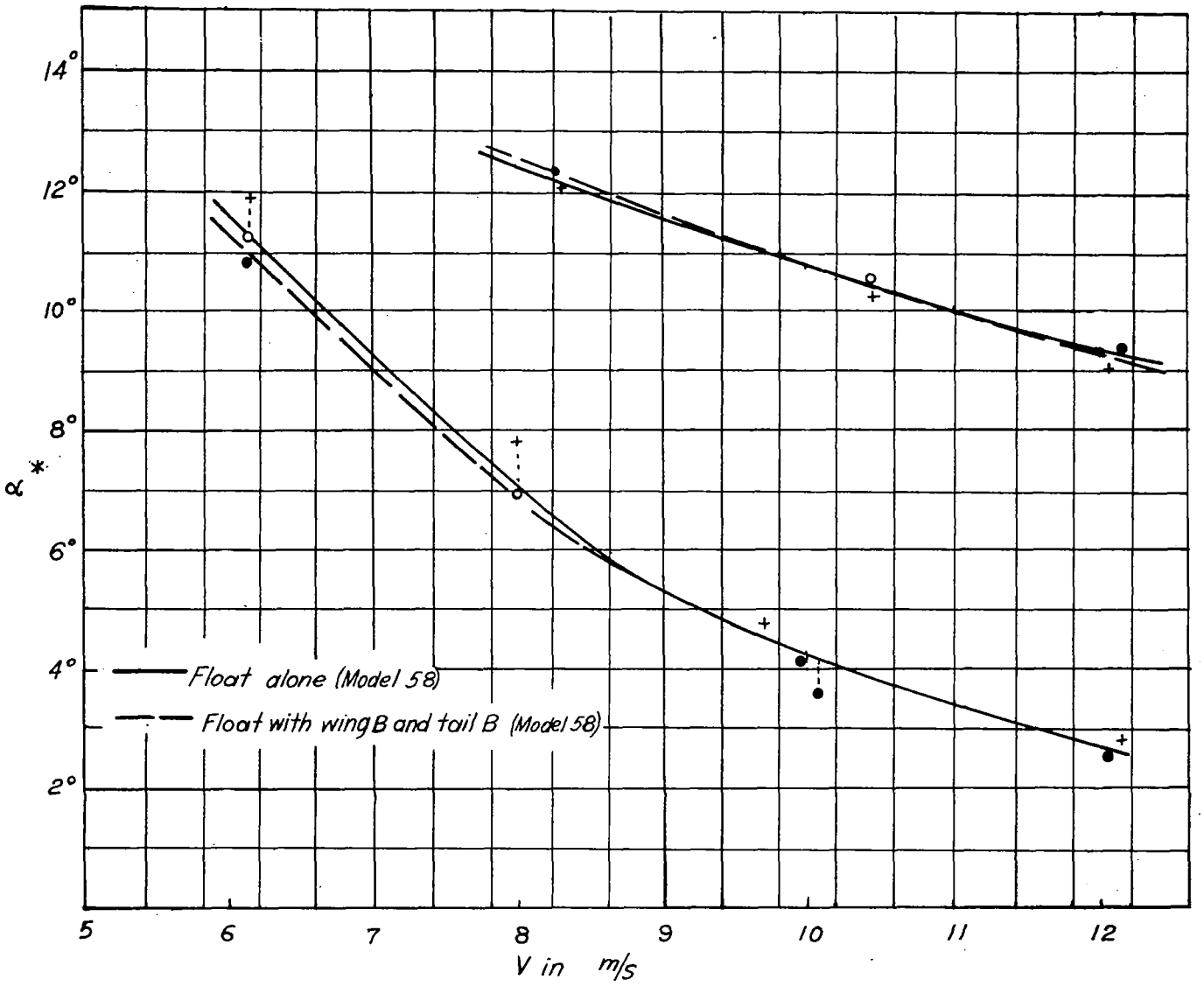

Figure 6.- Float design DVL 18 without wing and tail plane in comparison to the basic test.

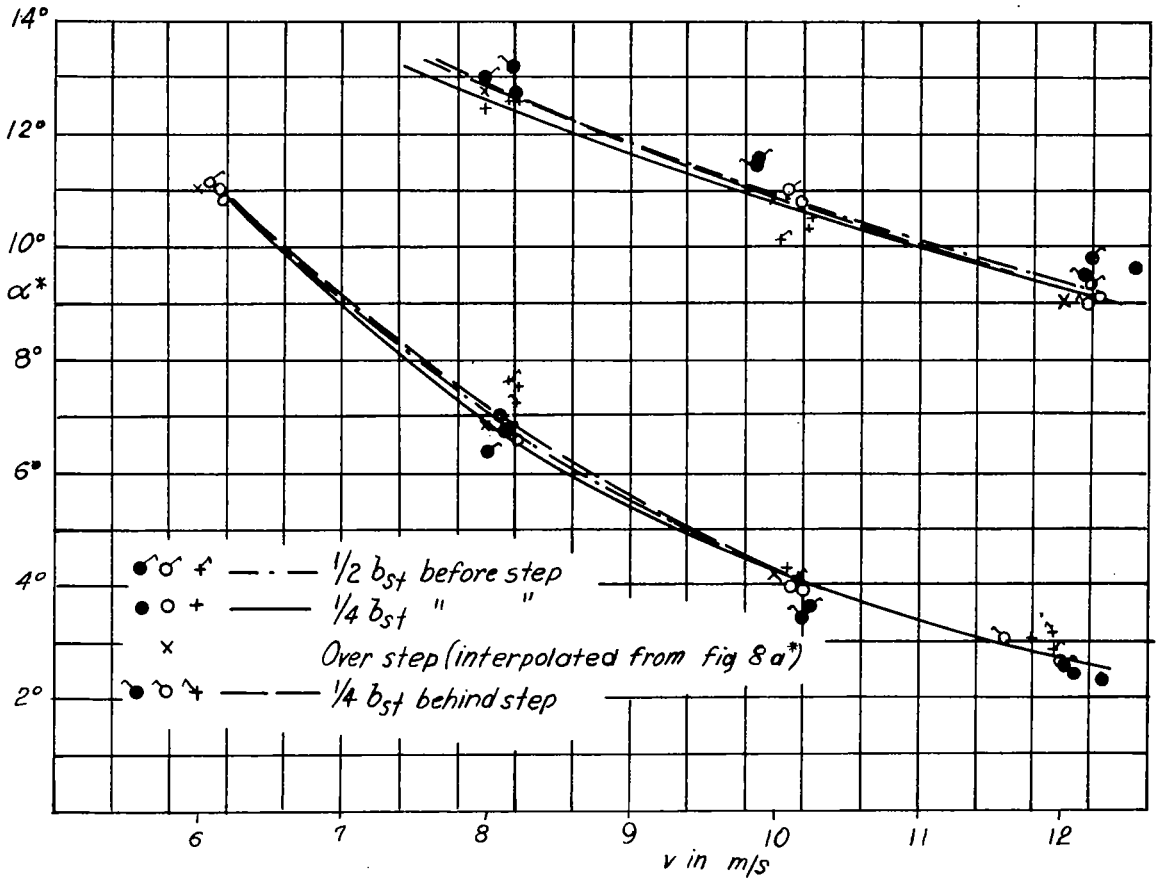

Figure 7.- Influence of the position of the center of gravity.

*The number of this figure was incorrect in the original version of this paper and has been corrected by the NACA reviewer.

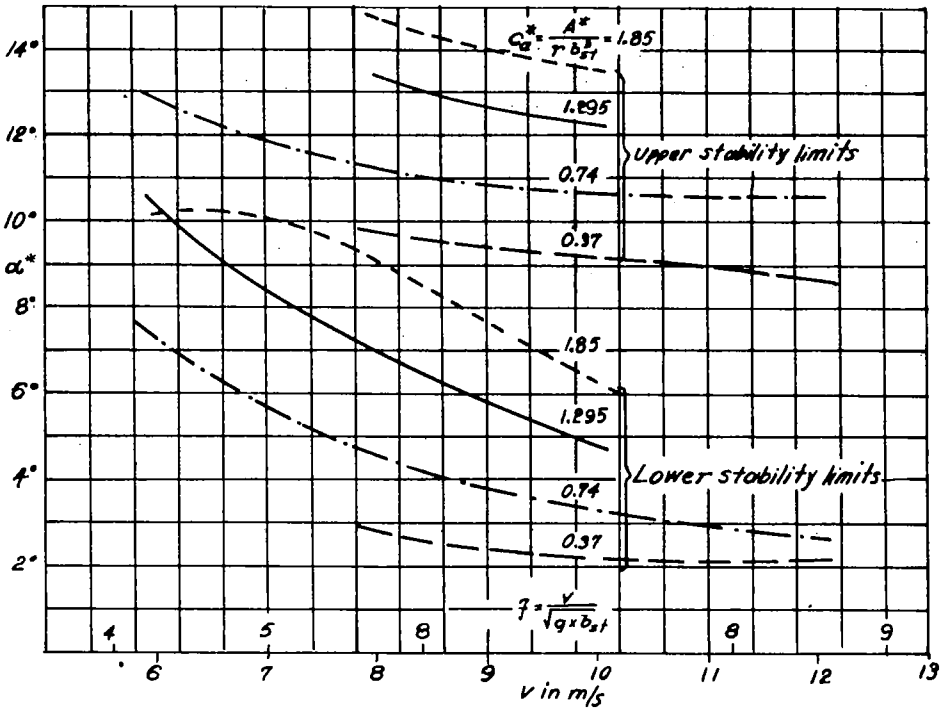

Figure 8.- Influence of the loading.

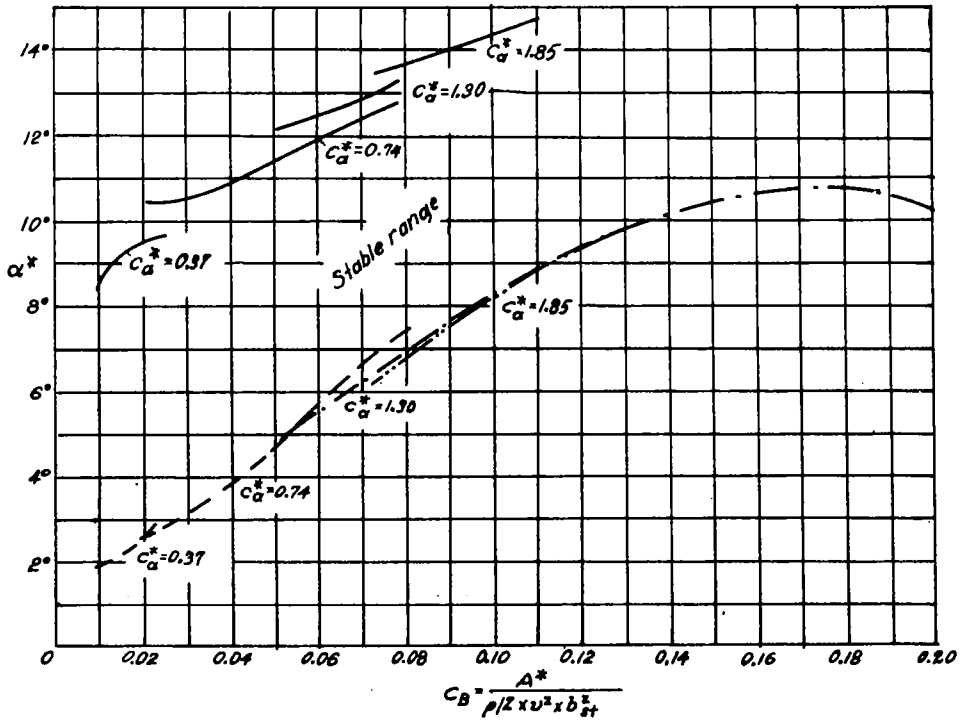

Figure 9.- Influence of the loading.

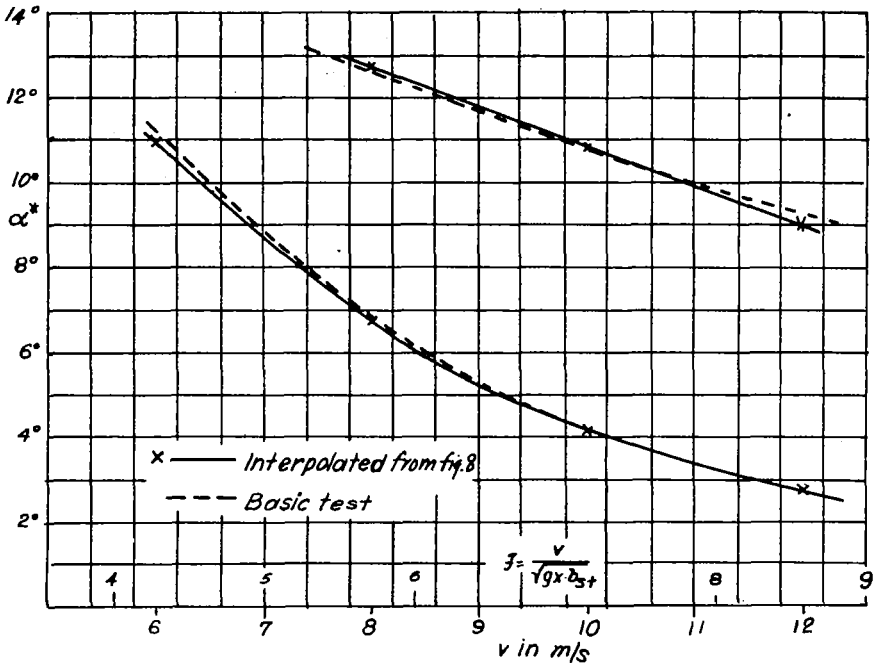

Figure 10.- Limits for direct and indirect towing method.

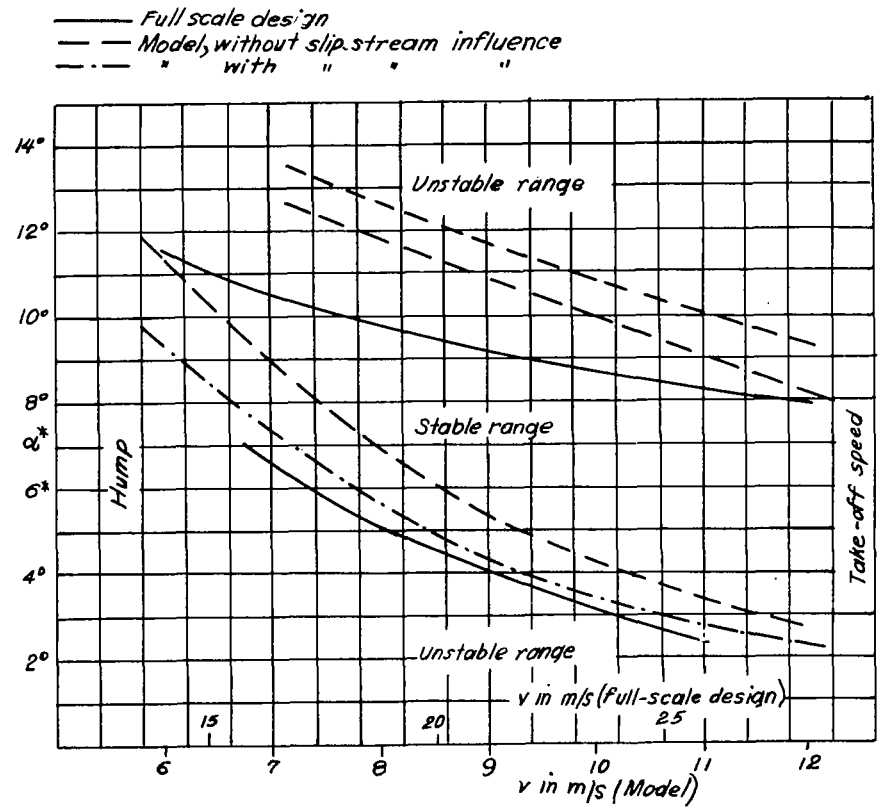

Figure 11.- Comparison between model and full-scale design.

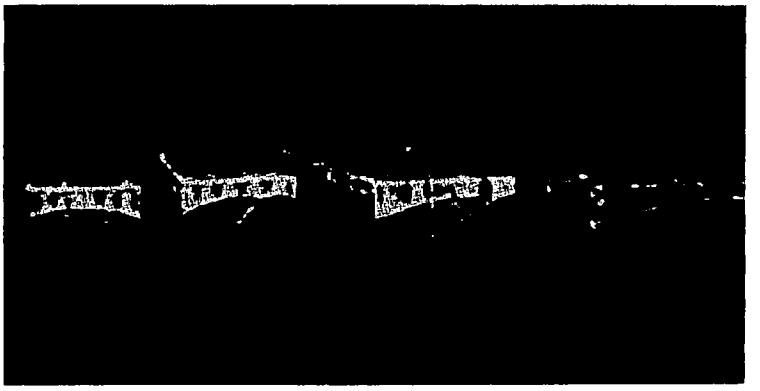

Figure 12.- Planing surfaces with 130°, 140°, 160°, and 180° keel angle.

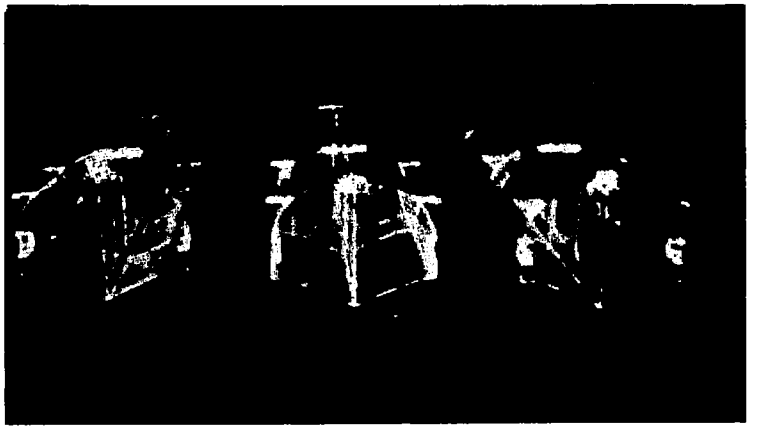

Figure 13.- Forebodies of the series of DVL float family of 130° keel angle.

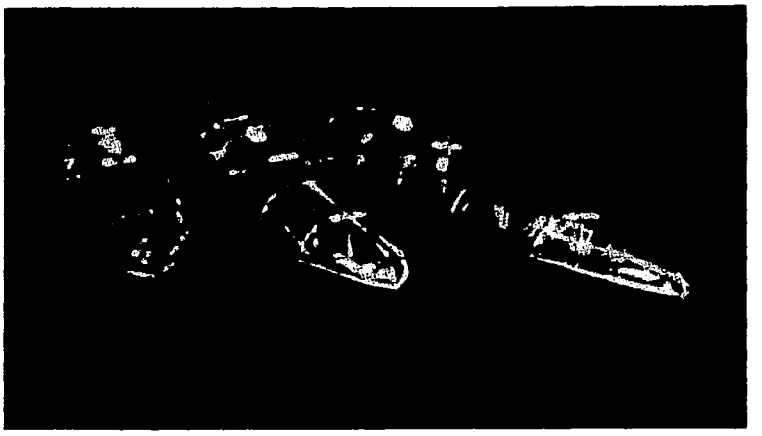

Figure 14.- Series of DVL float family of 130° keel angle.

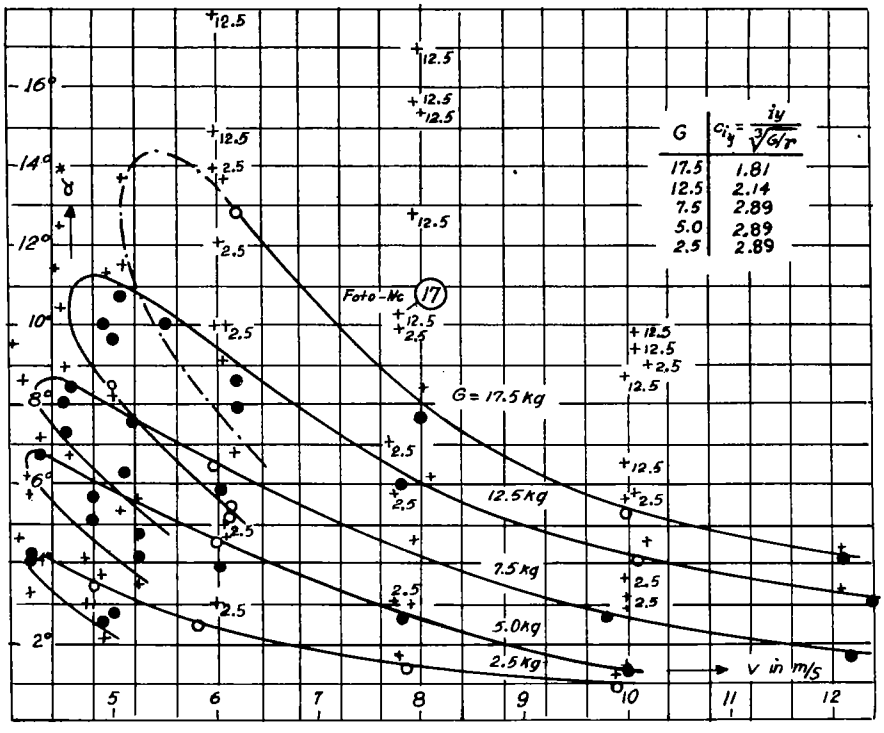

Figure 15.- Stability limits of the flat planing surface.

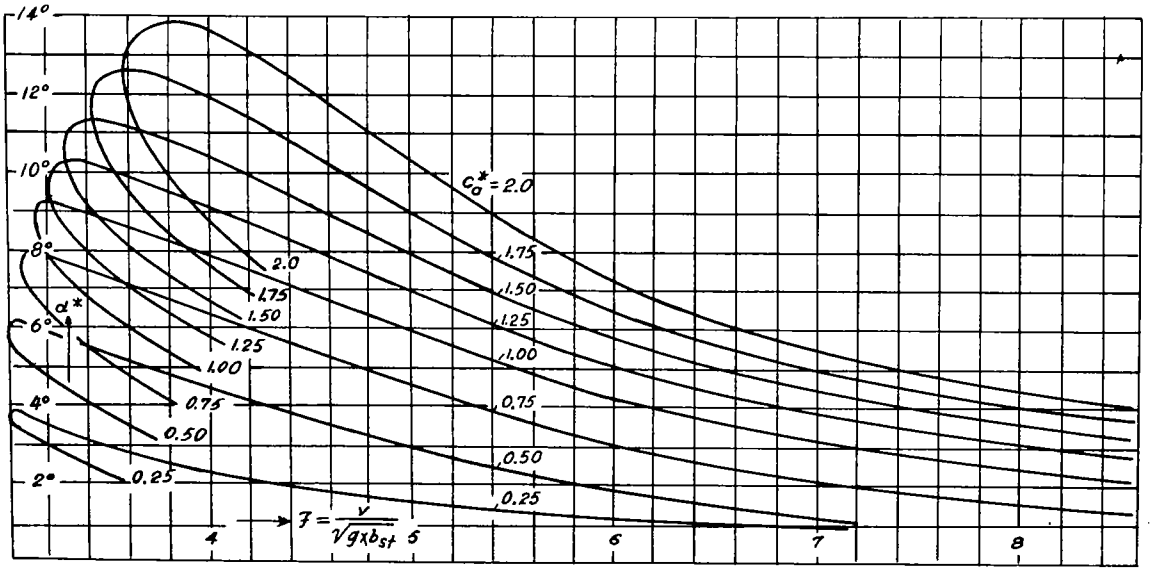

Figure 16.- Stability limits of the flat planing surface.

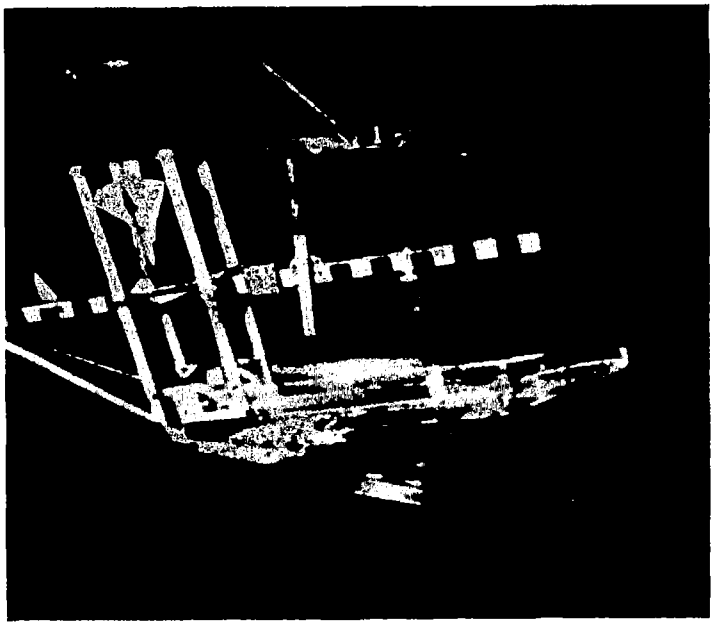

Figure 17.- Flat planing surface; $A^* = 12.5kg$, $\alpha^* = 10.2^{\circ}$, $v = 7.8m/s$ stable only for perfectly calm water; porpoising oscillations proper for slightly rippled water.

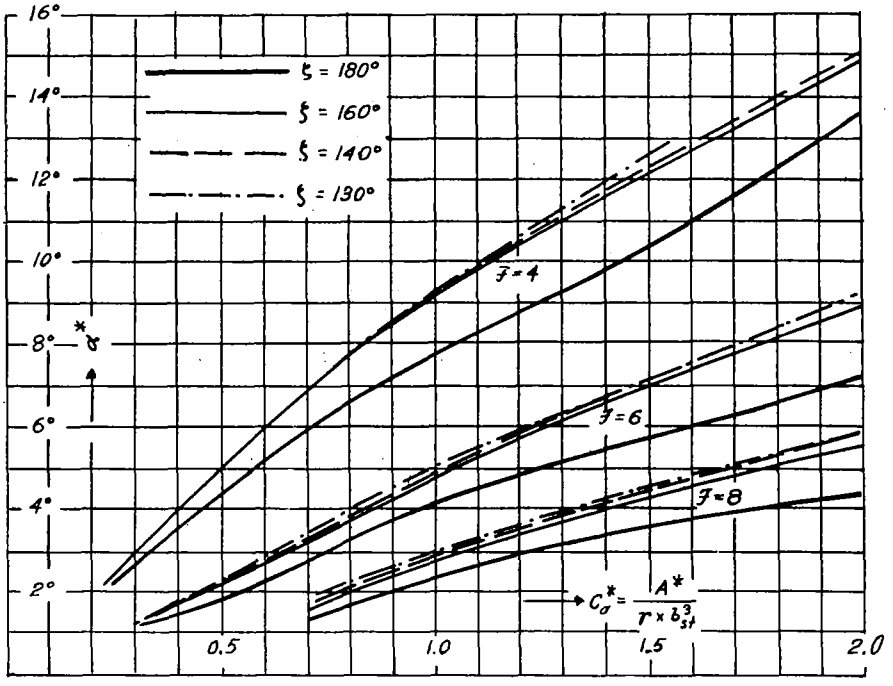

Figure 18.- Influence of the deadrise angle for planing surfaces.

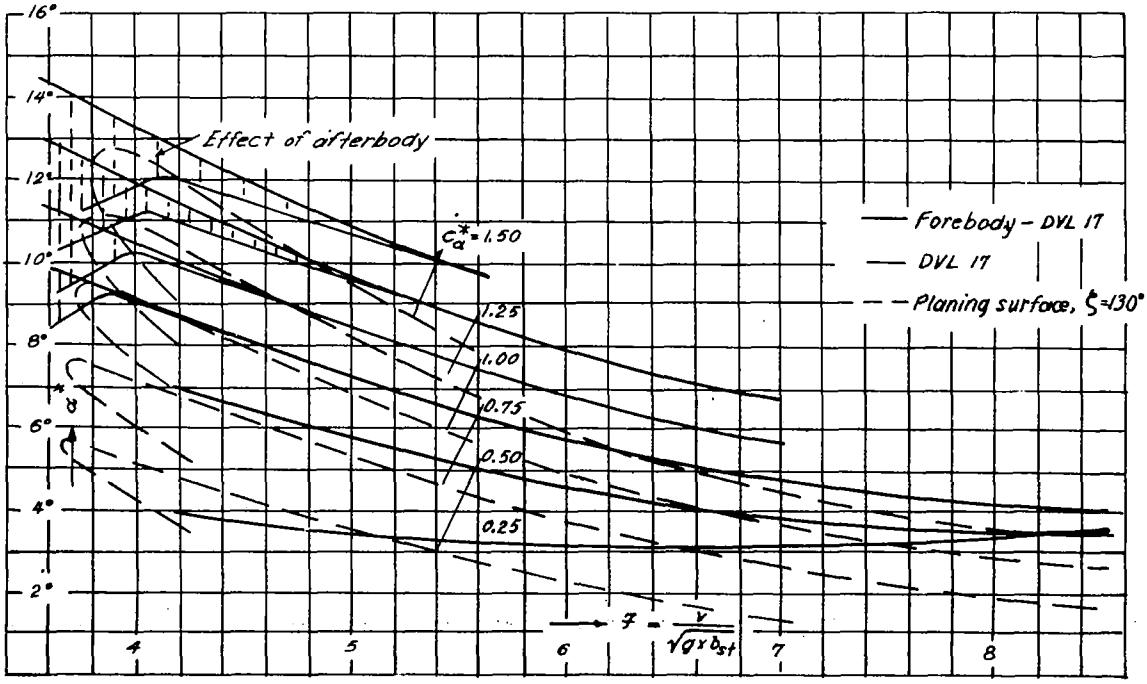

Figure 19.- Short forebody DVL 17; comparison with float DVL 17 and planing surface with 130° keel angle.

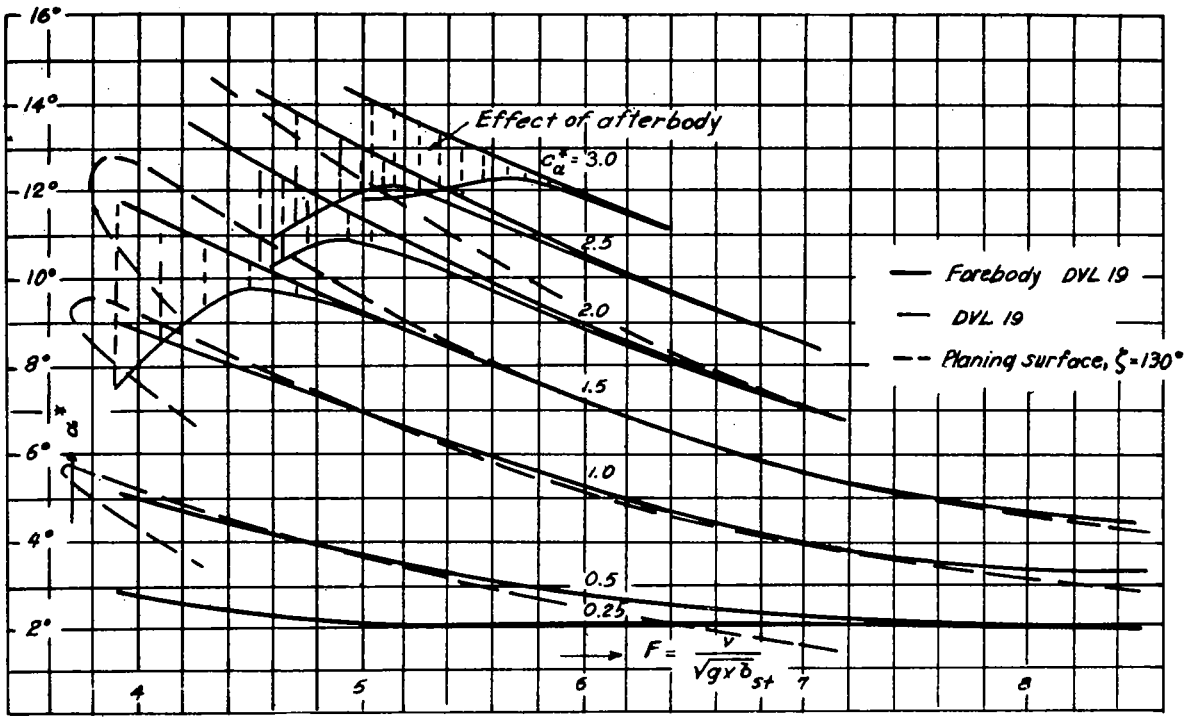

Figure 20.- Long forebody DVL 19; comparison with float DVL 19 and planing surface with 130° keel angle.

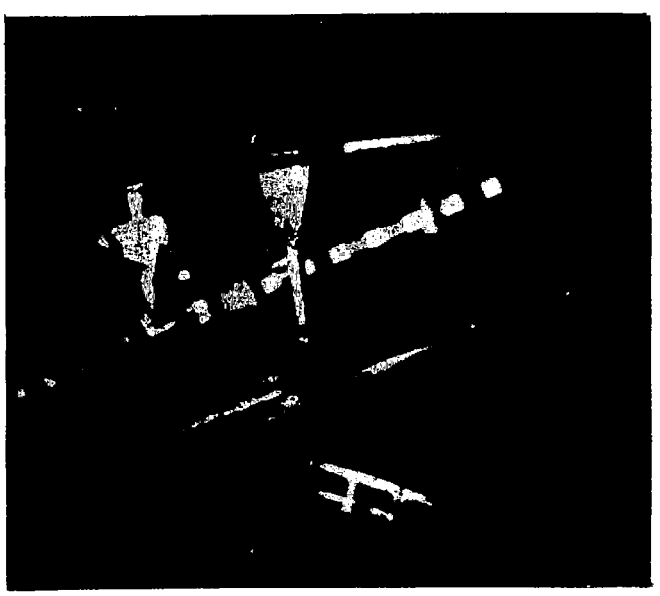

Figure 21.- Long forebody DVL 19; $A^* = 12.5$kg, $\alpha^* = 20°$, v = 5.5m/s stable even for high angle of attack.

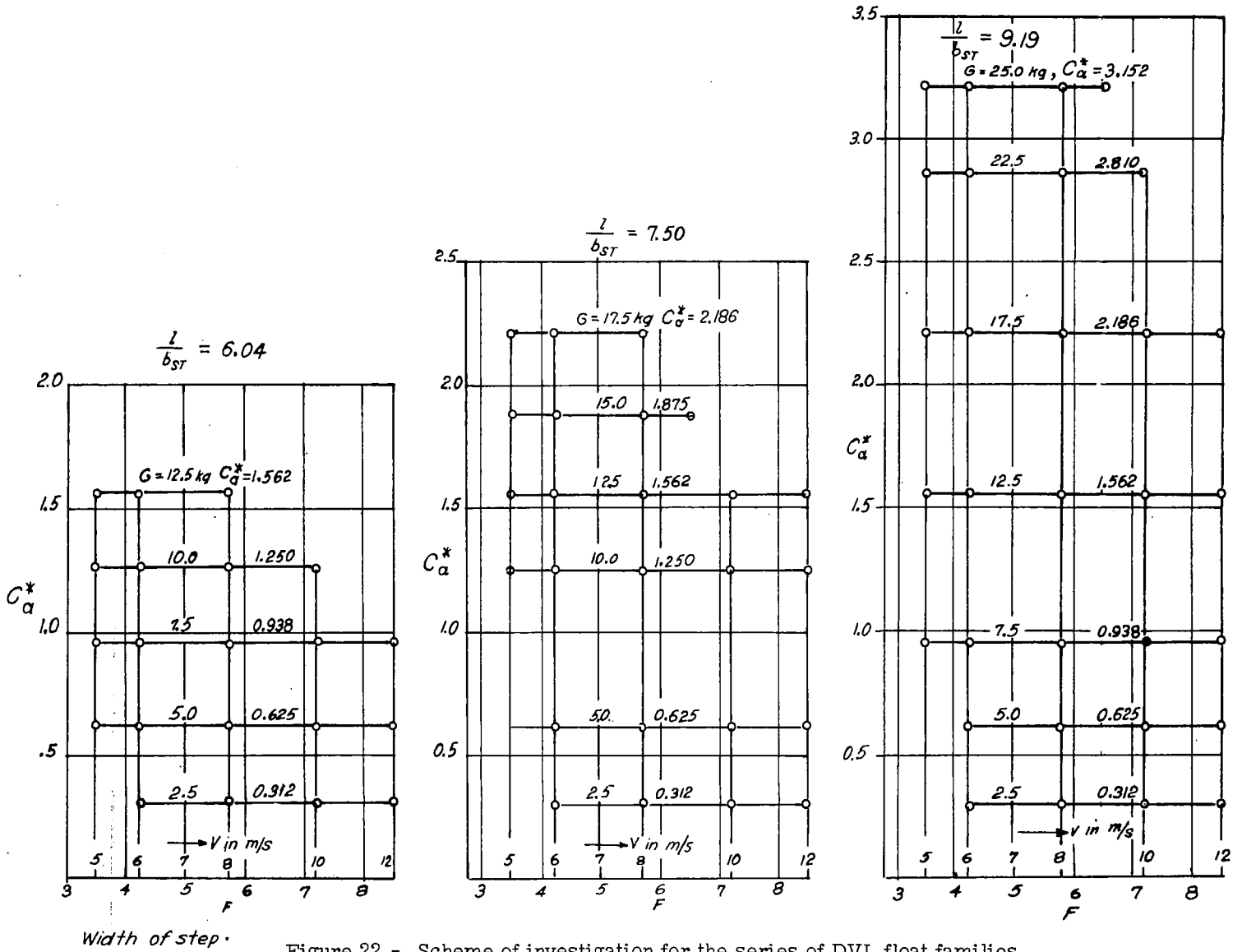

Figure 22.- Scheme of investigation for the series of DVL float families.

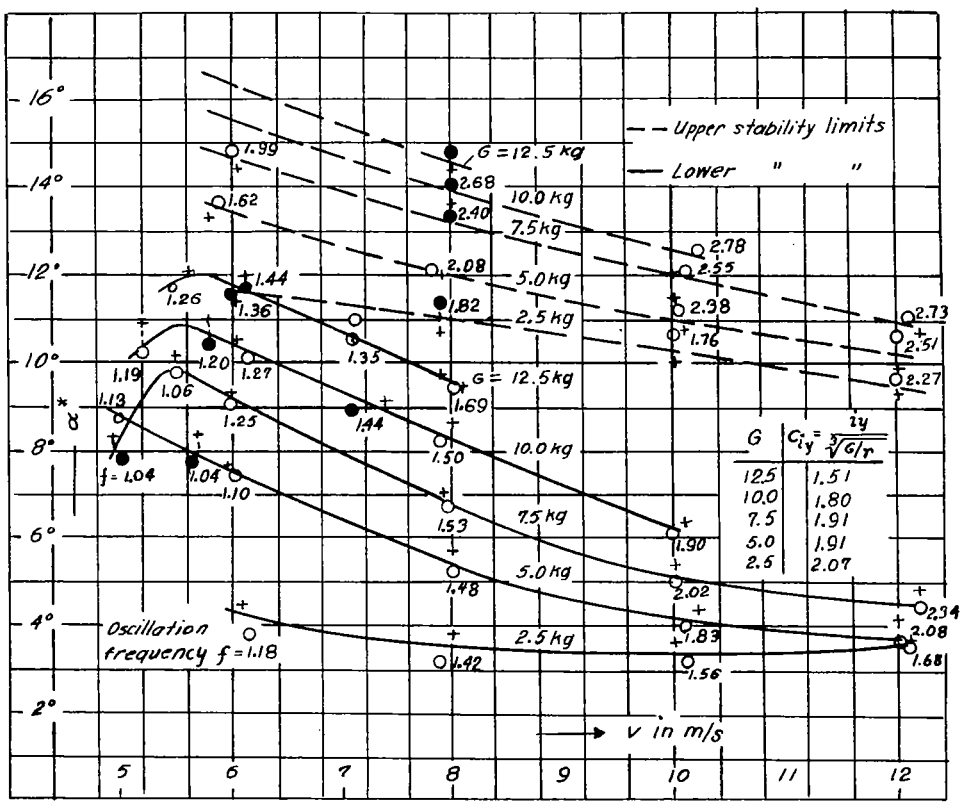

Figure 23.- Measured values for DVL 17, $\frac{l}{b_{st}} = 6.04$, $\zeta = 130°$.

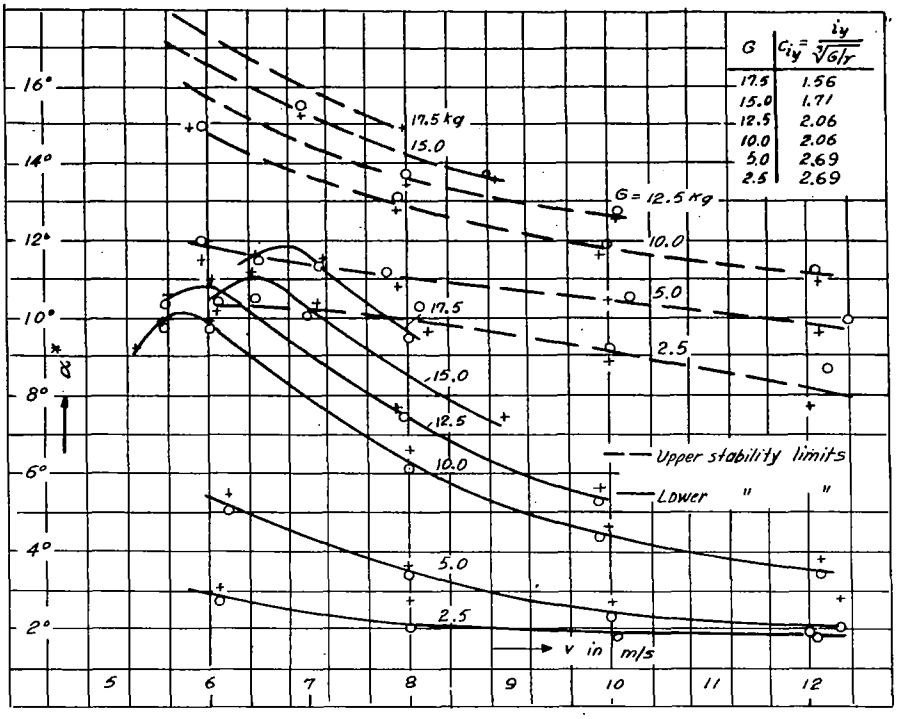

Figure 24.- Measured values for DVL 18, $\frac{l}{b_{st}} = 7.50$, $\zeta = 130°$.

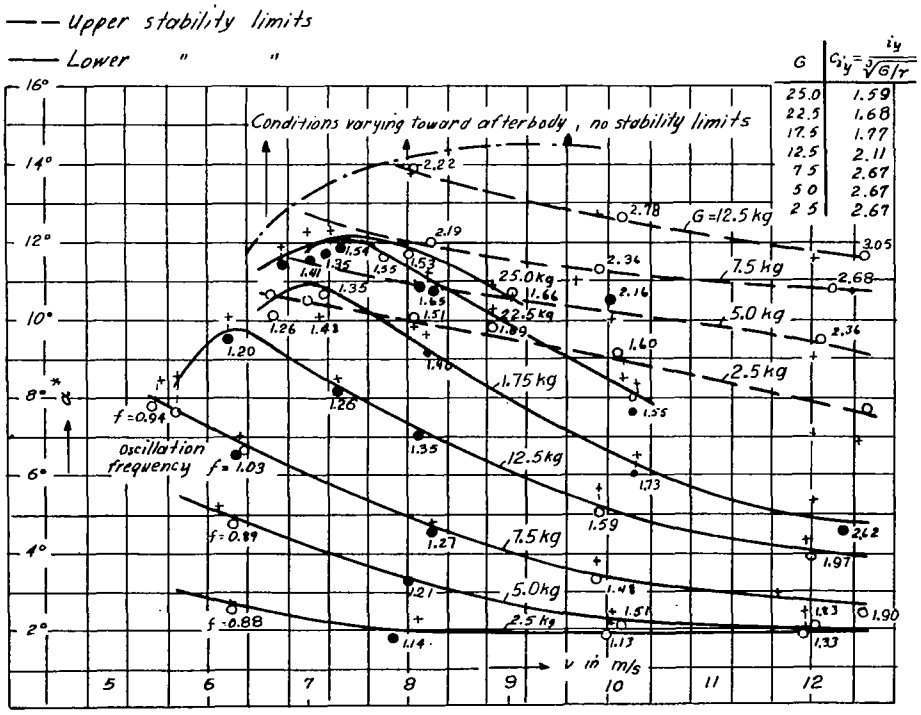

Figure 25.- Measured values for DVL 19, $\frac{l}{b_{st}} = 9.19$, $\zeta = 130°$.

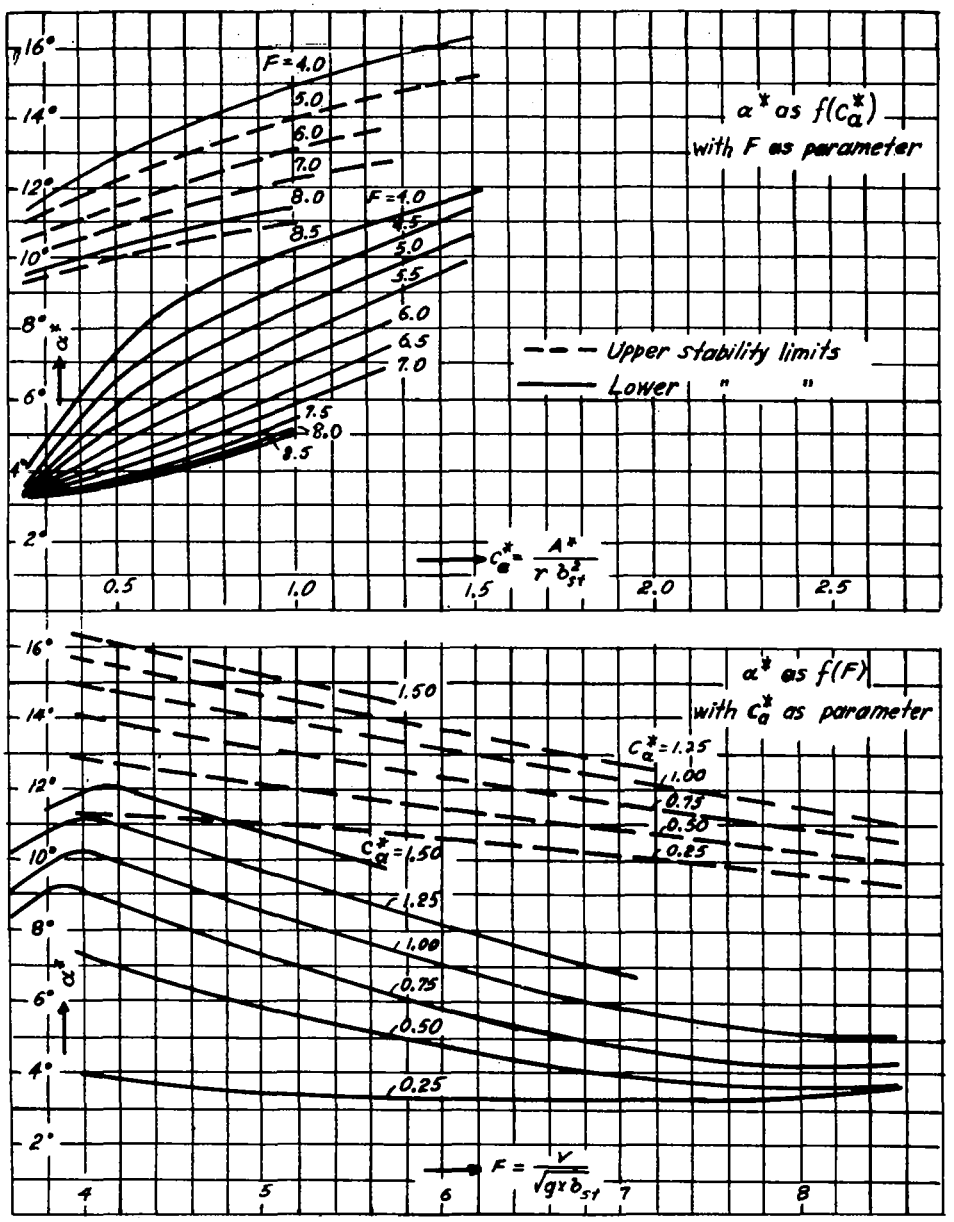

Figure 26.- Dimensionless work sheet for DVL 17, $\frac{l}{b_{st}} = 6.04$, $\zeta = 130^{\circ}$.

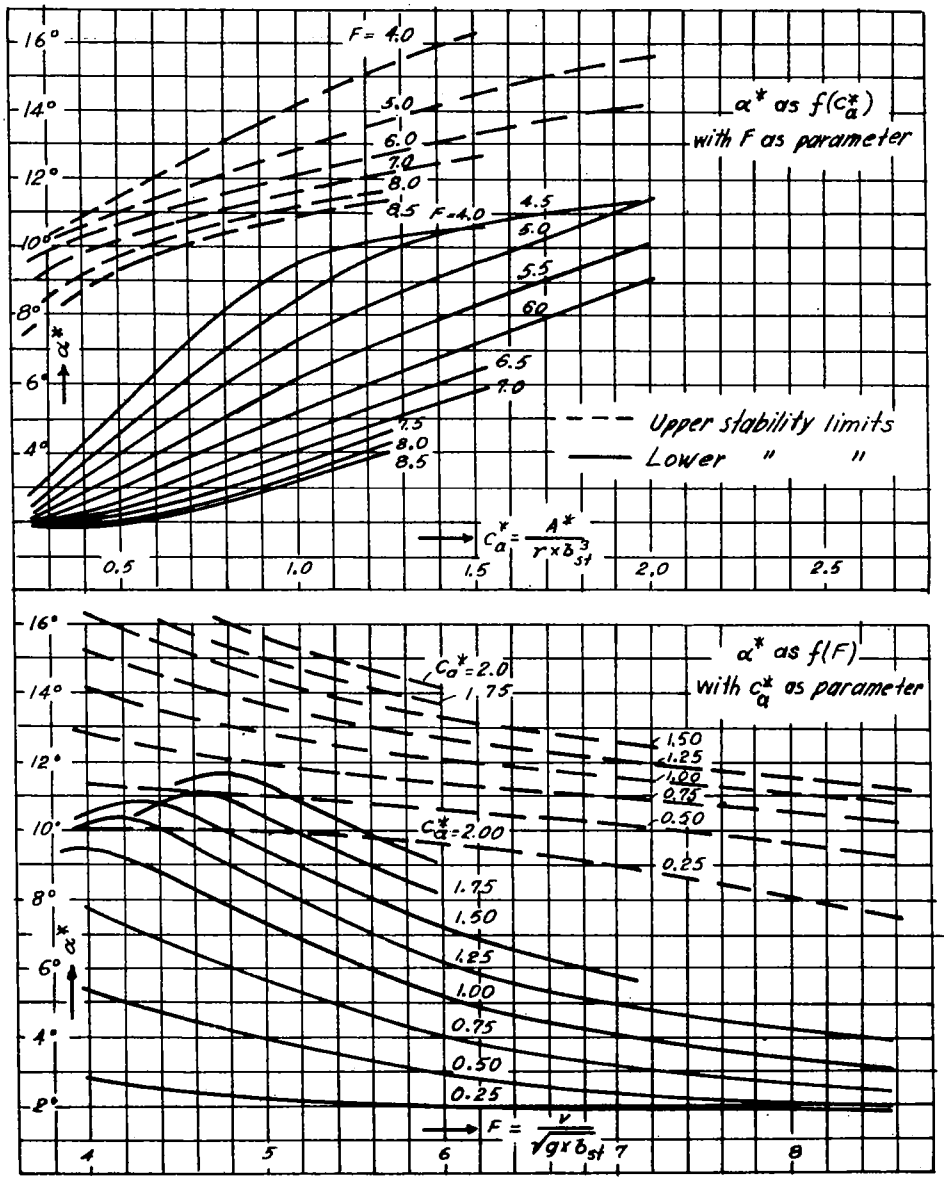

Figure 27.- Dimensionless work sheet for DVL 18, $\frac{l}{b_{st}} = 7.50$, $\zeta = 130^{\circ}$.

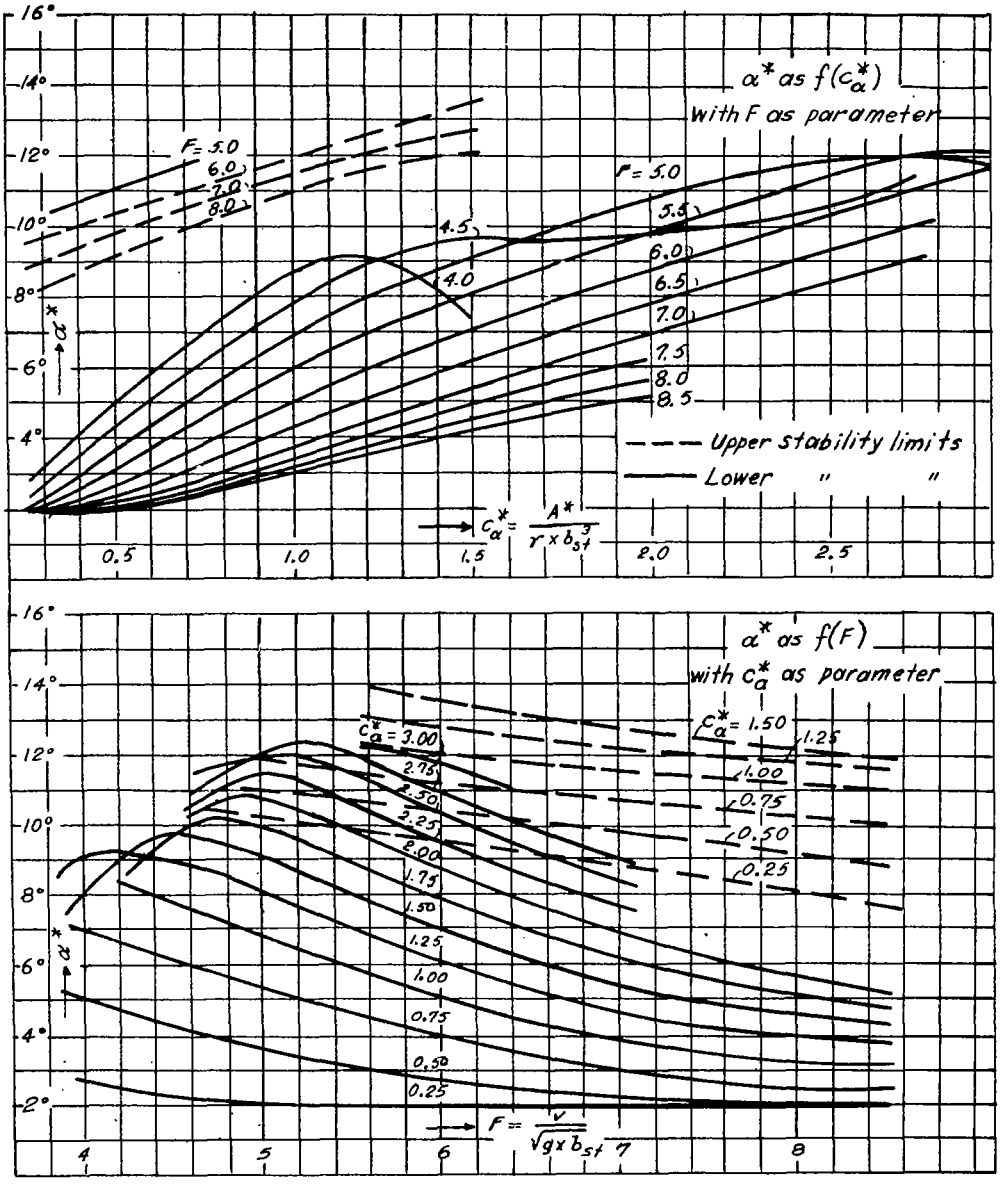

Figure 28.- Dimensionless work sheet for DVL 19, $\frac{l}{b_{st}} = 9.19$, $\zeta = 130^{\circ}$.

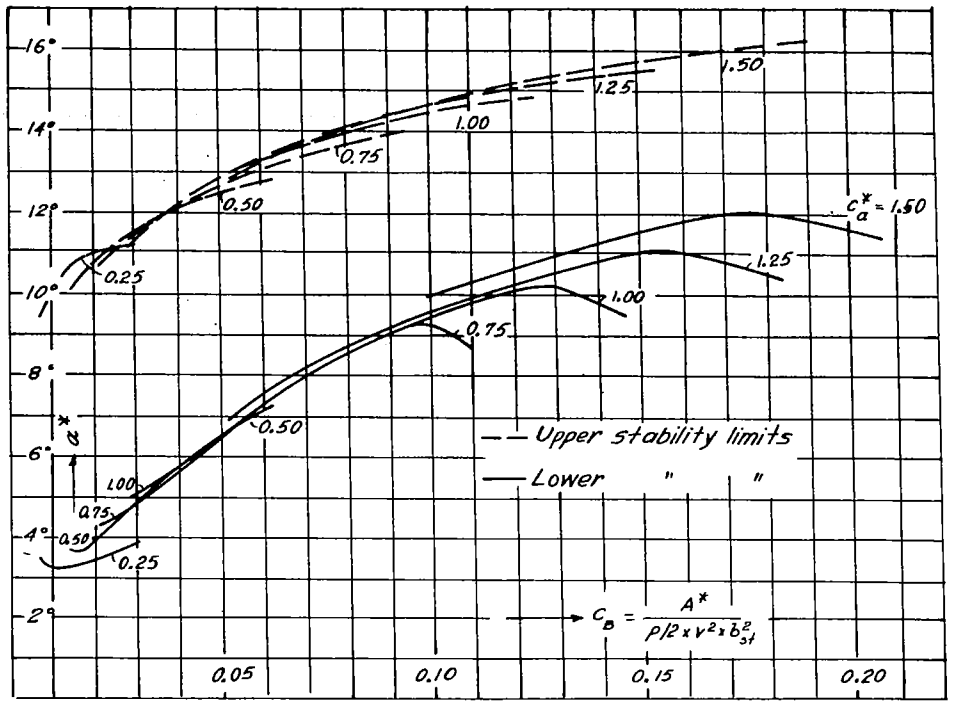

Figure 29.- α^* as $f(c_B)$ with c_a^* as parameter for DVL 17.

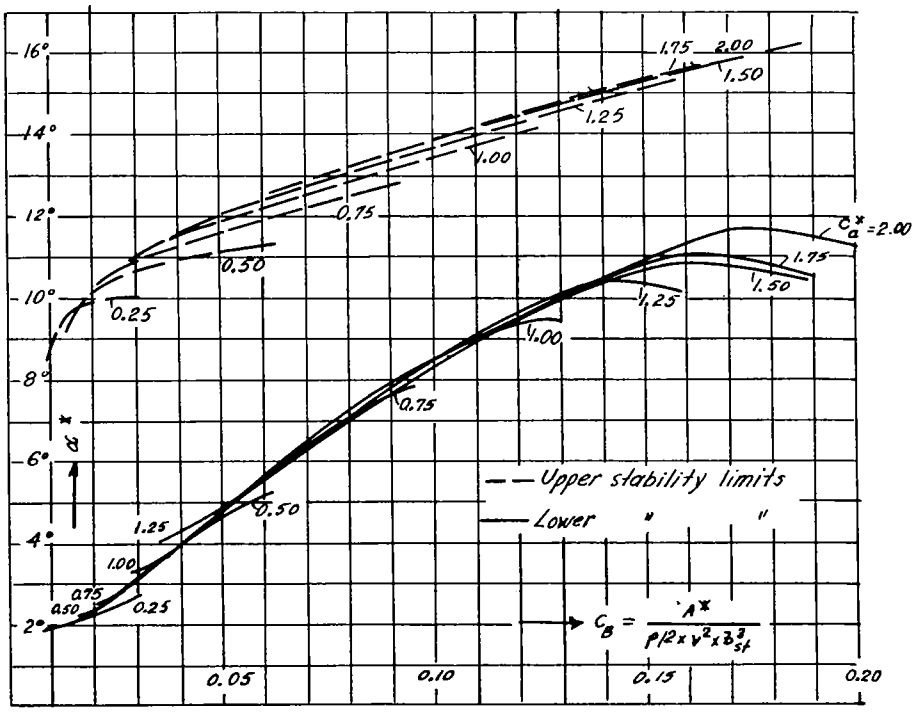

Figure 30.- α^* as $f(c_B)$ with c_a^* as parameter for DVL 18.

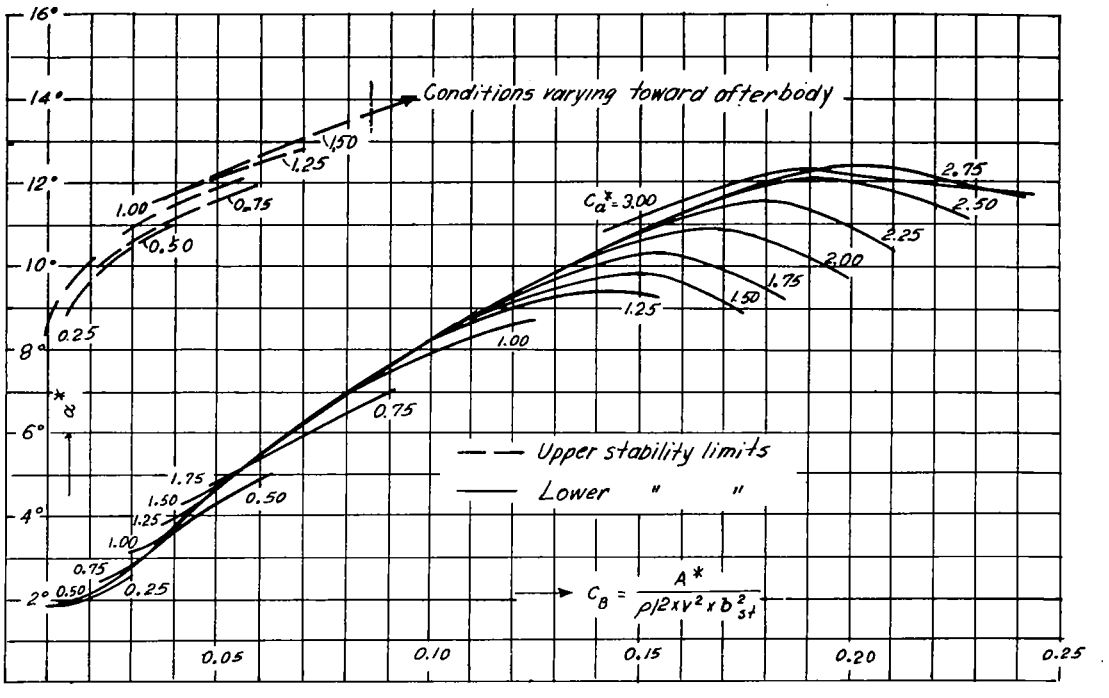

Figure 31.- α^* as $f(c_B)$ with c_a^* as parameter for DVL 19.

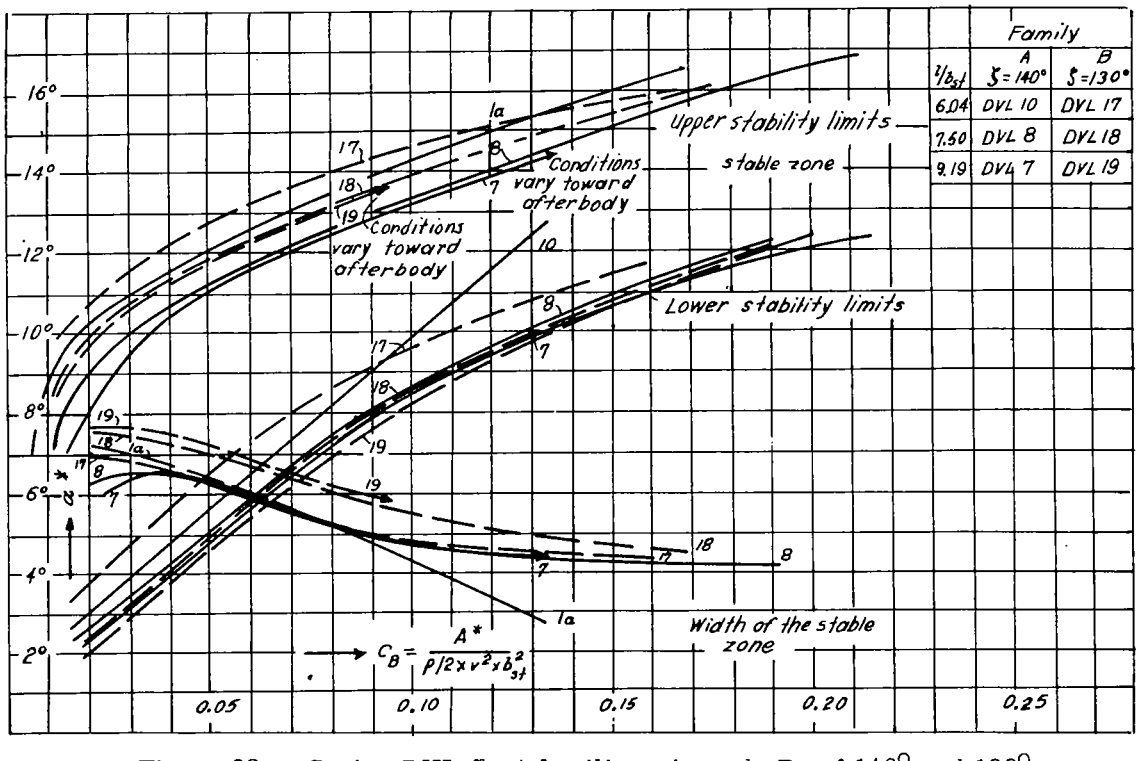

$1/b_{st}$	A $\zeta = 140°$	B $\zeta = 130°$
6.04	DVL 10	DVL 17
7.50	DVL 8	DVL 18
9.19	DVL 7	DVL 19

Figure 32.- Series DVL float families A and B of 140° and 130° keel angle; comparison of the mean stability limits.

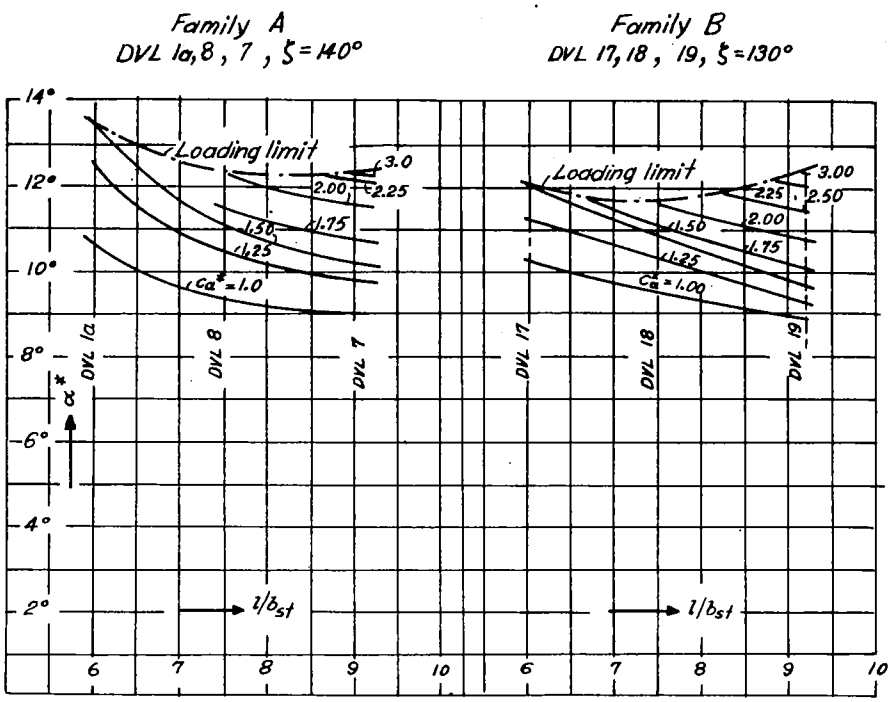

Figure 33.- Series DVL float families A and B of 140° and 130° keel angle; comparison of the stability maxima of the lower limit.

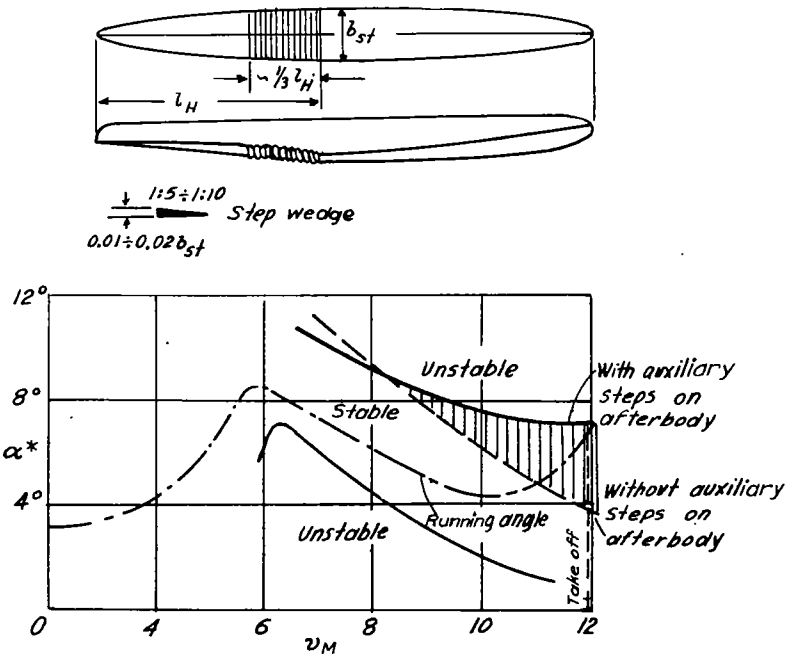

Figure 34.- Favorable shifting of the upper stability limit by use of auxiliary steps on the afterbody.

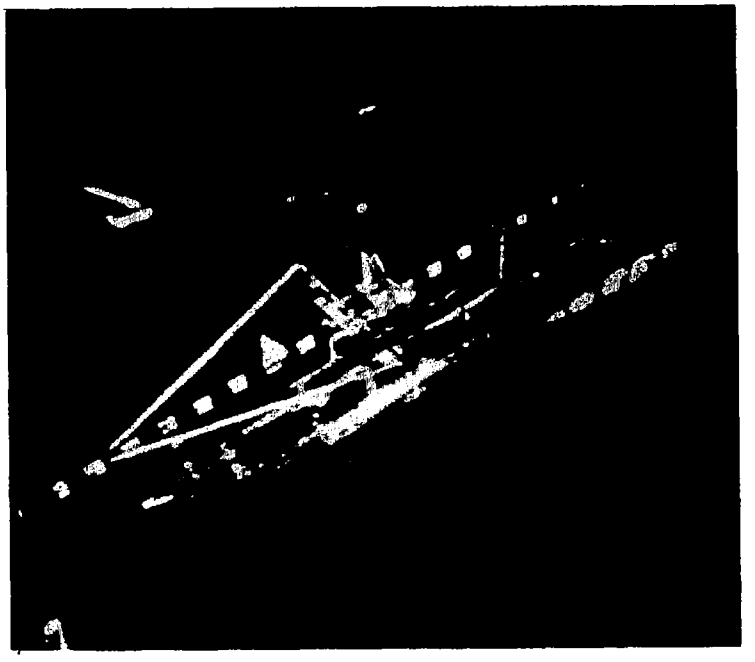

Figure 35.- Series of floats DVL 19 with auxiliary steps on afterbody; $A^* = 2.5k$, $\alpha^* = 8.2^\circ$, v = 12.5m/s, still stable at upper limit.

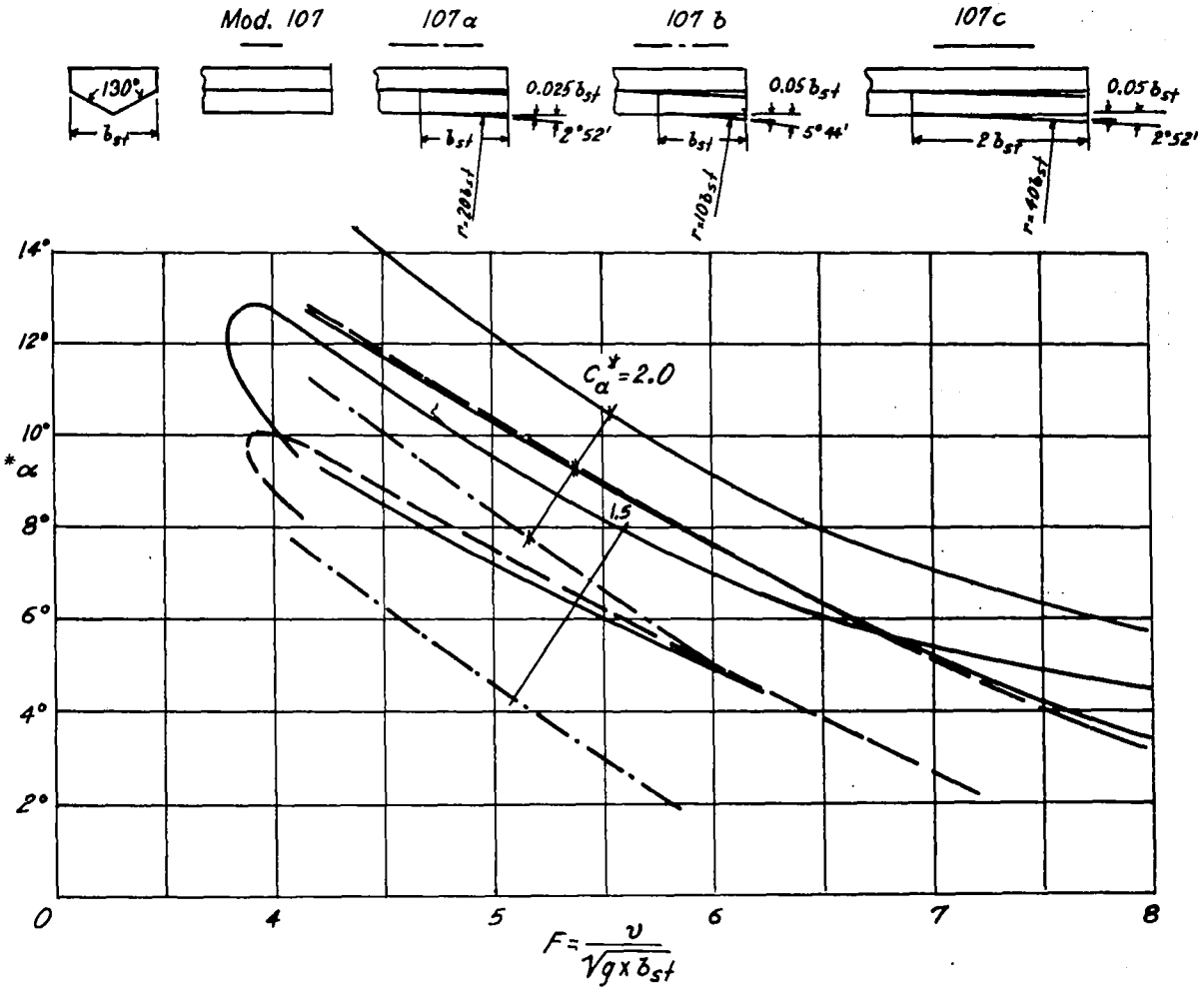

Figure 36.- Influence of a slight concavity of the bottom before the step on the position of the lower limit for the planing surface with a keel angle of 130°.